Cell Reports

Article

HIV Skews a Balanced Mtb-Specific Th17 Response in Latent Tuberculosis Subjects to a Pro-inflammatory Profile Independent of Viral Load

Graphical Abstract

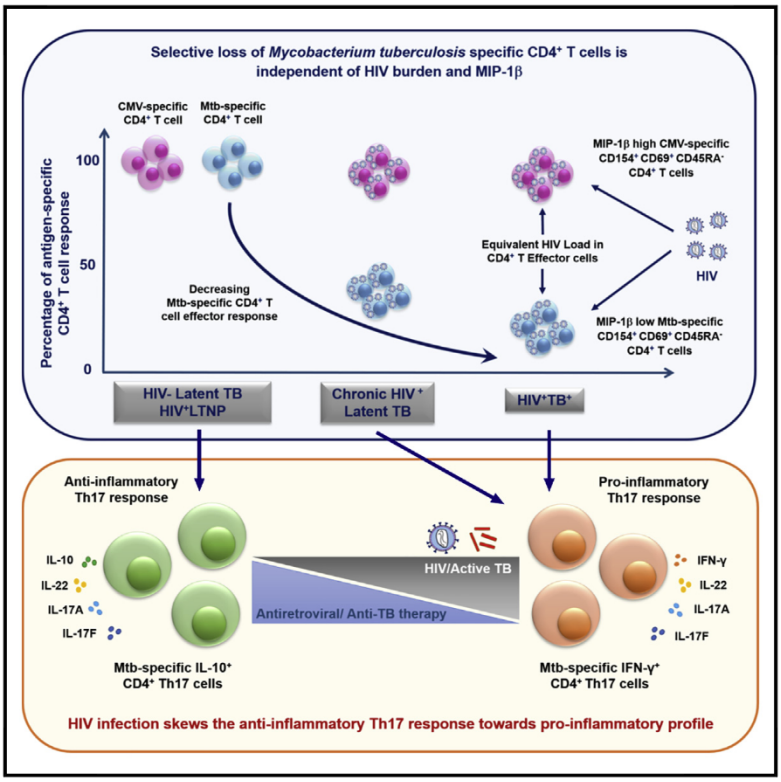

Highlights

- Chronic HIV infection selectively impairs Mtb-specific effector cytokine responses
- Chronic HIV infection augments Mtb-specific pro-inflammatory Th17 responses
- HIV-induced changes in Mtb-specific cells are independent of viral load and MIP-1β
- ART/ATT restore anti-inflammatory and dampen pro-inflammatory Th17 responses

Authors

Srabanti Rakshit, Nitin Hingankar, Shuba Varshini Alampalli, ..., Stephen C. De Rosa, Tom H.M. Ottenhoff, Annapurna Vyakarnam

Correspondence

anna.vyakarnam@kcl.ac.uk

In Brief

This study provides insight on how HIV may drive tuberculosis (TB). Rakshit et al. demonstrate that HIV infection of latent TB subjects profoundly alters specific immune subsets implicated in anti-TB immunity, which is independent of cellular viral burden or secretion of antiviral chemokines.

Rakshit et al., 2020, Cell Reports *33*, 108451
December 1, 2020
https://doi.org/10.1016/j.celrep.2020.108451

CellPress

Cell Reports

CellPress
OPEN ACCESS

Article

HIV Skews a Balanced Mtb-Specific Th17 Response in Latent Tuberculosis Subjects to a Pro-inflammatory Profile Independent of Viral Load

Srabanti Rakshit,[1] Nitin Hingankar,[1] Shuba Varshini Alampalli,[1] Vasista Adiga,[1] Bharath K. Sundararaj,[1] Pravat Nalini Sahoo,[1] Greg Finak,[2] Anto Jesuraj Uday Kumar J,[3] Chirag Dhar,[3] George D'Souza,[3] Rashmi Govind Virkar,[4] Manisha Ghate,[4] Madhuri R. Thakar,[4] Ramesh S. Paranjape,[4] Stephen C. De Rosa,[2] Tom H.M. Ottenhoff,[5] and Annapurna Vyakarnam[1,6,7,*]

[1]Laboratory of Immunology of HIV-TB Co-infection, Centre for Infectious Disease Research, Indian Institute of Science, Bangalore, India
[2]Vaccine and Infectious Disease Division, Fred Hutchinson Cancer Research Center, Seattle, WA, USA
[3]Departments of Infectious Diseases & Pulmonary Medicine, St. John's Research Institute, Bangalore, India
[4]National Aids Research Institute, Bhosari, Pune, Maharashtra, India
[5]Department of Infectious Diseases, Leiden University Medical Center, Leiden, the Netherlands
[6]Peter Gorer Department of Immunobiology, School of Immunology and Microbial Sciences, Faculty of Life Sciences & Medicine, Guy's Hospital, King's College London, London SE1 9RT, UK
[7]Lead Contact
*Correspondence: anna.vyakarnam@kcl.ac.uk
https://doi.org/10.1016/j.celrep.2020.108451

SUMMARY

HIV infection predisposes latent tuberculosis-infected (LTBI) subjects to active TB. This study is designed to determine whether HIV infection of LTBI subjects compromises the balanced *Mycobacterium tuberculosis* (Mtb)-specific T helper 17 (Th17) response of recognized importance in anti-TB immunity. Comparative analysis of Mtb- and cytomegalovirus (CMV)-specific $CD4^+$ T cell responses demonstrates a marked dampening of the Mtb-specific $CD4^+$ T cell effectors and polyfunctional cells while preserving CMV-specific response. Additionally, HIV skews the Mtb-specific Th17 response in chronic HIV-infected LTBI progressors, but not long-term non-progressors (LTNPs), with preservation of pro-inflammatory interferon (IFN)-γ^+/interleukin-17^+ (IL-17^+) and significant loss of anti-inflammatory IL-10^+/IL-17^+ effectors that is restored by anti-retroviral therapy (ART). HIV-driven impairment of Mtb-specific response cannot be attributed to preferential infection as cell-associated HIV DNA and HIV RNA reveal equivalent viral burden in $CD4^+$ T cells from different antigen specificities. We therefore propose that beyond HIV-induced loss of Mtb-specific $CD4^+$ T cells, the associated dysregulation of Mtb-specific T cell homeostasis can potentially enhance the onset of TB in LTBI subjects.

INTRODUCTION

AIDS and tuberculosis (TB) are among the top 10 leading causes of death worldwide. The interaction between the two causative pathogens, HIV and *Mycobacterium tuberculosis* (Mtb), exacerbates disease pathology and substantially contributes to this high incidence of mortality (Diedrich and Flynn, 2011). In 2018, globally 38 million people were estimated to be HIV^+, of which 862,000 were diagnosed as TB^+. Furthermore, TB is the leading cause of death among people with HIV, accounting for one-third of HIV-related deaths; i.e., 251,000 of 770,000 people died from HIV-associated TB in 2018 according to World Health Organization (WHO) reports (WHO, 2019a; WHO, 2019b). Healthy subjects with latent TB infection (LTBI) are reportedly identified by the QuantiFERON TB gold in-tube interferon gamma release assay (IGRA) and commonly referred to as either LTBI or $IGRA^+$ (henceforth referred to as $IGRA^+$) (Auguste et al., 2017). Although the majority of $IGRA^+$ subjects remain asymptomatic over their lifetime, 5%–15% progress to active disease manifested either as pulmonary TB (PTB) in the lung or extrapulmonary TB (EPTB) in the lymph nodes, pleura, abdomen, and other organs (Lin and Flynn, 2018). Chronic HIV infection enhances the risk of TB reactivation by >20-fold and annual incidence by 5%–15% (Pawlowski et al., 2012; Bell and Noursadeghi, 2018) that is reduced by 67% in anti-retroviral therapy (ART)-treated $IGRA^+$ subjects (Lawn and Wilkinson, 2015). Conversely, increased incidence of TB in $IGRA^+$ HIV-infected long-term non-progressors (LTNPs), who are defined as remaining asymptomatic for at least 7 years following infection with preserved CD4 T cell counts despite being viremic and not on ART (Ciccone et al., 2011), has not been reported. Hence, deciphering the mechanisms by which HIV infection predisposes $IGRA^+$ subjects to TB is an area of significant scientific and global health interest.

Insight on immune mechanisms by which HIV may drive TB disease have emerged from both human studies and from non-human primate (NHP) models of HIV-TB coinfection. Reactivation of TB in NHPs is not likely solely governed by reduced $CD4^+$ T cell counts induced by HIV infection but depends on

other immune factors, including macrophage disruption (Kuroda et al., 2018) and absence of granzyme-positive $CD8^+$ T cells (Foreman et al., 2016). Human studies, in contrast, highlight both HIV-induced $CD4^+$ T cell depletion and functional changes of Mtb-specific $CD4^+$ T cells to be major factors by which HIV drives TB incidence (Douek et al., 2003; Geldmacher et al., 2010; Okoye and Picker, 2013; Esmail et al., 2018; Murray et al., 2018; Amelio et al., 2019). Understanding the precise functional changes that HIV infection of humans induces in the Mtb-specific T cell response is therefore important. Several phenotypic and functional studies highlight selective vulnerability of Mtb-specific $CD4^+$ T cells to HIV infection. Effector memory $CD4^+$ T cells that express the HIV entry receptor CCR5 are dramatically depleted in the gut, which serves as a major *in vivo* reservoir of infection (Yang et al., 2012). Importantly, $CD4^+$ memory T cells primed to recognize Mtb and HIV antigens express elevated levels of HIV entry coreceptor CCR5 and conversely low levels of the anti-HIV chemokine macrophage inflammatory protein (MIP)-1β, which binds CCR5 and blocks HIV entry; these cells are consequently highly susceptible to HIV infection, whereas memory cells specific for cytomegalovirus (CMV), an opportunistic pathogen that emerges late in HIV infection, are poorly infected linked to high MIP-1β expression and lower CCR5 expression (Geldmacher et al., 2010; Geldmacher and Koup, 2012; Bronke et al., 2005). Moreover, Mtb-specific $CD4^+$ T cells display an early differentiated phenotype with enhanced proliferation potential due to higher interleukin-2 (IL-2) production, making them more permissive to HIV infection than the terminally differentiated CMV-specific $CD4^+$ T cells (Ahmed et al., 2016). Additionally, cytokine imbalance and loss of polyfunctional Mtb-specific $CD4^+$ T cells are also associated with HIV-infected IGRA status (Amelio et al., 2019; Day et al., 2008, 2017; Riou et al., 2016).

Within the CD4 compartment, a major focus is to understand how HIV alters the Mtb-specific T helper 17 (Th17) responses based on substantial recent evidence highlighting $CD4^+$ Th17 cells, which otherwise are important in maintaining gut mucosa integrity, to play crucial roles in protective immunity against HIV and Mtb infection (Esmail et al., 2018). Th17 cells exhibit considerable heterogeneity and plasticity as they can differentiate into distinct subsets in the presence of specific cytokine milieu. Naive $CD4^+$ T cells cultured in the presence of transforming growth factor β (TGF-β) and IL-6 differentiate into regulatory and protective Th17 that co-express of IL-17 and IL-10, while the additional presence of IL-1β and/or IL-23 steers them toward the pro-inflammatory and pathogenic Th17 cells that co-express of IL-17 and interferon (IFN)-γ (Mercer et al., 2014). Moreover, Mtb-specific memory cells in $IGRA^+$ subjects are mostly contained within the $CXCR3^+CCR6^+CD4^+$ T cell subset that express both IFN-γ and IL-17 and represent the pathogenic phenotype (Acosta-Rodriguez et al., 2007). Furthermore, $CCR4^+CCR6^+$ Th17 and $CXCR3^+CCR6^+$ (Th1/Th17) cells that express the HIV coreceptors CCR5 and CXCR4 and secrete low levels of MIP-1β are highly susceptible to *in vitro* infection by R5 and X4 HIV viruses (Elhed and Unutmaz, 2010; Gosselin et al., 2010). Additionally, these Th17 subsets also exhibit gut- and lymph node-homing potential that might relate to their significant depletion in the gastrointestinal tract of chronic HIV-infected individuals (Bixler and Mattapallil, 2013), but not in HIV-infected LTNPs (Ciccone et al., 2011; Caetano et al., 2020).

Data from our laboratory have provided the first evidence of the potential importance of a balanced Mtb-specific Th17 response in TB immunity. We demonstrated the presence of Mtb-specific regulatory or anti-inflammatory $IL\text{-}17^+$ cells that co-expressed IL-10 in $IGRA^+$ subjects, while subjects with TB showed significant loss of this subset while preserving Mtb-specific pro-inflammatory $IL\text{-}17^+$ cells that co-expressed IFN-γ (Rakshit et al., 2017). Additionally, sterile granulomas in a TB NHP model were associated with increased T cells producing both IL-10 and IL-17 (Gideon et al., 2015). Importantly, protective immunity to Mtb infection induced by Bacillus Calmette-Guérin (BCG) vaccination in a live challenge NHP model was associated with IL-10- and Mtb-specific Th17 $CD4^+$ T cells (Dijkman et al., 2019). In our recent study involving young human adults, we showed that BCG revaccination has the potential to enhance Mtb-specific $IL\text{-}17^+$ cells that co-expressed IL-10, but not $IL\text{-}17^+$ cells that co-expressed IFN-γ (Rakshit et al., 2019). The aim of this study was therefore to investigate the impact of HIV infection on the nature of the Mtb-specific Th17 response. We hypothesized that HIV infection of $IGRA^+$ subjects would alter the balance of Mtb-specific Th17 pro- versus anti-inflammatory $IL\text{-}17^+$ cells, skewing the response to a pro-inflammatory phenotype previously noted in subjects with TB (Rakshit et al., 2017), thereby potentially predisposing $IGRA^+$ subjects to TB disease progression. We provide evidence in support of our hypothesis through a comparative analysis of immune profiles combined with HIV load analyses in $CD4^+$ T cells specific for Mtb versus CMV in $IGRA^+$ subjects with progressive HIV disease versus HIV^+IGRA^+ LTNPs and subjects with TB with and without chronic HIV infection before and after ART or anti-TB treatment (ATT).

RESULTS

HIV Infection Significantly Reduces the Absolute Numbers of Total Mtb-Specific $CD4^+$ T Cells in $IGRA^+$ Individuals

HIV Infection leads to the functional impairment of Mtb-specific $CD4^+$ and $CD8^+$ T cell responses (Amelio et al., 2019); however, the precise mechanisms by which HIV hampers the Mtb-specific $CD4^+$ T cell response are poorly understood. To address this issue, we first compared the absolute numbers of Mtb-specific $CD4^+$ T cells in subjects from the following four clinical groups: HIV^+IGRA^+ versus HIV^-IGRA^+ and HIV^+IGRA^- versus HIV^-IGRA^- with all HIV^+ subjects displaying significantly lower absolute CD4 T cell counts than the HIV-uninfected counterpart group (see Table 1). Representative fluorescence-activated cell sorting (FACS) plots depicting the complete stepwise gating strategy to identify functional subsets are shown in Figure S1. Comparison of HIV^-IGRA^+ versus HIV^+IGRA^+ subjects (green versus red plots) would assess the impact of chronic HIV infection on Mtb-specific responses of $IGRA^+$ subjects, while a comparison of HIV^-IGRA^- versus HIV^+IGRA^- subjects (brown versus blue plots) would determine the impact of chronic HIV infection independent of IGRA status (Figures 1A and 1B). We measured the expression of six key effector cytokines, namely IFN-γ, IL-2, MIP-1β, tumor necrosis factor alpha (TNF-α), IL-10, and IL-17F, in response to

Table 1. Information of Study Groups and Participants

Group	N	Sex[a]	Age (Median/ Range)	CD4 Count (Median/ Range)	Viral Load (Median/ Range)
HIV$^-$IGRA$^-$	10	M = 4; F = 6	28 (20–39)	M: 822 (381–1,565)[b]; F: 953 (447–1,846)	NA
HIIV$^-$IGRA$^+$	10	M = 8; F = 2	30 (25–38)	M: 822 (381–1,565)[b]; F: 953 (447–1,846)	NA
HIV$^+$IGRA$^-$	10	M = 7; F = 3	31 (24–47)	433.5 (230–721)	37,300 (2,840–131,000)
HIV$^+$IGRA$^+$	10	M = 5; F = 5	37.5 (27–56)	352 (289–540)	27,926 (3,510–516,564)
HIV$^+$IGRA$^+$ LTNP[c]	7	M = 3; F = 4	36.5 (33–48)	823 (679–1,259)	9,943 (0–19,897)
HIV$^+$IGRA$^+$/IGRA$^-$ 1 year post ART	9	M = 4; F = 5	32 (24-56)	484 (282–524)	not detected or <40
Pulmonary TB BL & 6 months post ATT	5	M = 4; F = 1	34 (30–66)	M: 822 (381–1,565)[b]; F: 953 (447–1,846)	NA
Extrapulmonary TB BL & 6 months post ATT	3	M = 2; F = 1	25 (17–45)	M: 822 (381–1,565)[b]; F: 953 (447–1,846)	NA
HIV-TB	8	M = 7; F = 1	37 (23–67)	1,495 (64–259)	194,500 (26,200–1,160,000)

NA, not applicable.
[a]M, male; F, female.
[b]Thakar et al. (2011).
[c]Kulkarni et al. (2017).

the Mtb ESAT6/CFP10 fusion protein (referred to as EC) and to a pool of four Mtb DosR latency antigens (Rv1733c, Rv1737c, Rv2029, and Rv2628), referred to as LT Ag in CD4$^+$ T cells. These antigens were selected based on previous studies showing responses to the LT Ag, in particular to clearly distinguish asymptomatic IGRA$^+$ subjects from those with active TB disease (Rakshit et al., 2017; Coppola and Ottenhoff, 2018). To determine whether HIV infection impacted recall responses, we compared the Mtb-specific response with that of CMV. Unlike TB, which is evident at all stages of HIV infection, CMV emerges late in HIV infection as an opportunistic pathogen concomitant with profound CD4$^+$ T cell loss. Mitogen-driven (phytohemagglutinin [PHA]) responses were measured to evaluate the impact on global T cell responses, irrespective of cell specificity. Representative flow cytometry plots depict total effector cytokine expression by CD4$^+$ T cells to different antigenic stimuli relative to unstimulated negative control (Figure S2).

Figures S3A and S3B show the total frequencies of cytokine-positive CD4$^+$ T cells enumerated, and in Figures 1A and 1B, the same data are represented as absolute CD4$^+$ numbers corrected for individual donors' CD4$^+$ T cell counts, thereby enabling an accurate estimation of specific CD4$^+$ T cell changes across subjects with wide variations in their circulating CD4$^+$ T cell numbers (see Table 1). We record significant reduction in all cytokine subsets specific for both EC and LT Ag in HIV$^+$IGRA$^+$ (red) versus HIV$^-$IGRA$^+$ (green), with the exception of IL-10 (Figure 1A). Consistent with lower or minimal Mtb antigenic burden in IGRA$^-$ compared with IGRA$^+$ subjects (Carpenter et al., 2015), the IGRA$^-$ groups, HIV$^+$ (blue) and HIV$^-$ (brown) on the whole had lower absolute numbers of these Mtb-specific CD4$^+$ T cells compared with their IGRA$^+$ counterparts (red and green), (Figures 1A and 1B). Except for TNF-α, the downward trend noticed in the absolute numbers of most cytokines to EC stimulation did not reach statistical significance; neither were there any appreciable differences in absolute numbers of cytokines to LT Ag stimulation in HIV$^+$IGRA$^-$ compared with HIV$^-$IGRA$^-$ subjects (Figure 1B). In keeping with previous data (Geldmacher et al., 2010), a marked 10-fold reduction in MIP-1β was noted in Mtb-specific cells from the IGRA$^+$ group, whereas an increase in the absolute numbers of MIP-1β^+ CMV-specific CD4$^+$ T cells was observed in IGRA$^-$ subjects following HIV infection (Figures 1A and 1B). With the exception of MIP-1β, all other effector cytokine responses measured to CMV and PHA stimulation were similar across all subjects tested, providing strong evidence that HIV infection had the potential to selectively impair Mtb-specific recall responses in IGRA$^+$ subjects (Figures 1A and 1B). These changes observed in absolute numbers of effector cytokine-positive CD4$^+$ T cells concurred with changes in cytokine frequencies (see Figures S3A and S3B). We also evaluated the impact of HIV infection on Mtb-specific CD8$^+$ T cell responses. Figure S3C shows no significant differences in the total frequencies of Mtb-specific CD8$^+$ T cells expressing IFN-γ and TNF-α in HIV-uninfected versus -infected subjects. However, absolute numbers of EC-specific CD8$^+$ T cells expressing IFN-γ in HIV$^+$IGRA$^+$ and the LT Ag-specific CD8$^+$ T cells expressing TNF-α in HIV$^+$IGRA$^-$ subjects were significantly enhanced compared with their respective HIV$^-$ counterparts (Figure S3D). Our CD8 data are broadly consistent with other human studies showing no significant changes in frequencies of EC-specific CD8$^+$IFN-γ^+ T cells in HIV-infected individuals irrespective of IGRA status or CD4 T cell counts (Murray et al., 2018; Kalokhe et al., 2015), with the increase in absolute number of cytokine-positive CD8$^+$ T cells in HIV$^+$IGRA$^+$ subjects likely due to the recognized HIV-infection-induced increase in blood CD8 T cell counts (Chiacchio et al., 2018). The absolute numbers of CMV-specific total IFN-γ^+ and TNF-α^+ CD4$^+$ and CD8$^+$ T cells, for all study participants, has been provided in Figure S4. Consistent with previous reports showing CMV recall responses to be well preserved (Chiacchio et al., 2018; Murray et al., 2018), we demonstrate a high proportion of CMV-specific CD4$^+$ (100%) and CD8$^+$ (80%–90%) T cell responders in the subjects recruited to our study (Figure S4).

HIV Infection Reduces the Polyfunctional Mtb-Specific Response of IGRA$^+$ Subjects

Mtb-specific, central memory polyfunctional responses are an important hallmark of IGRA$^+$ subjects (Rakshit et al., 2017;

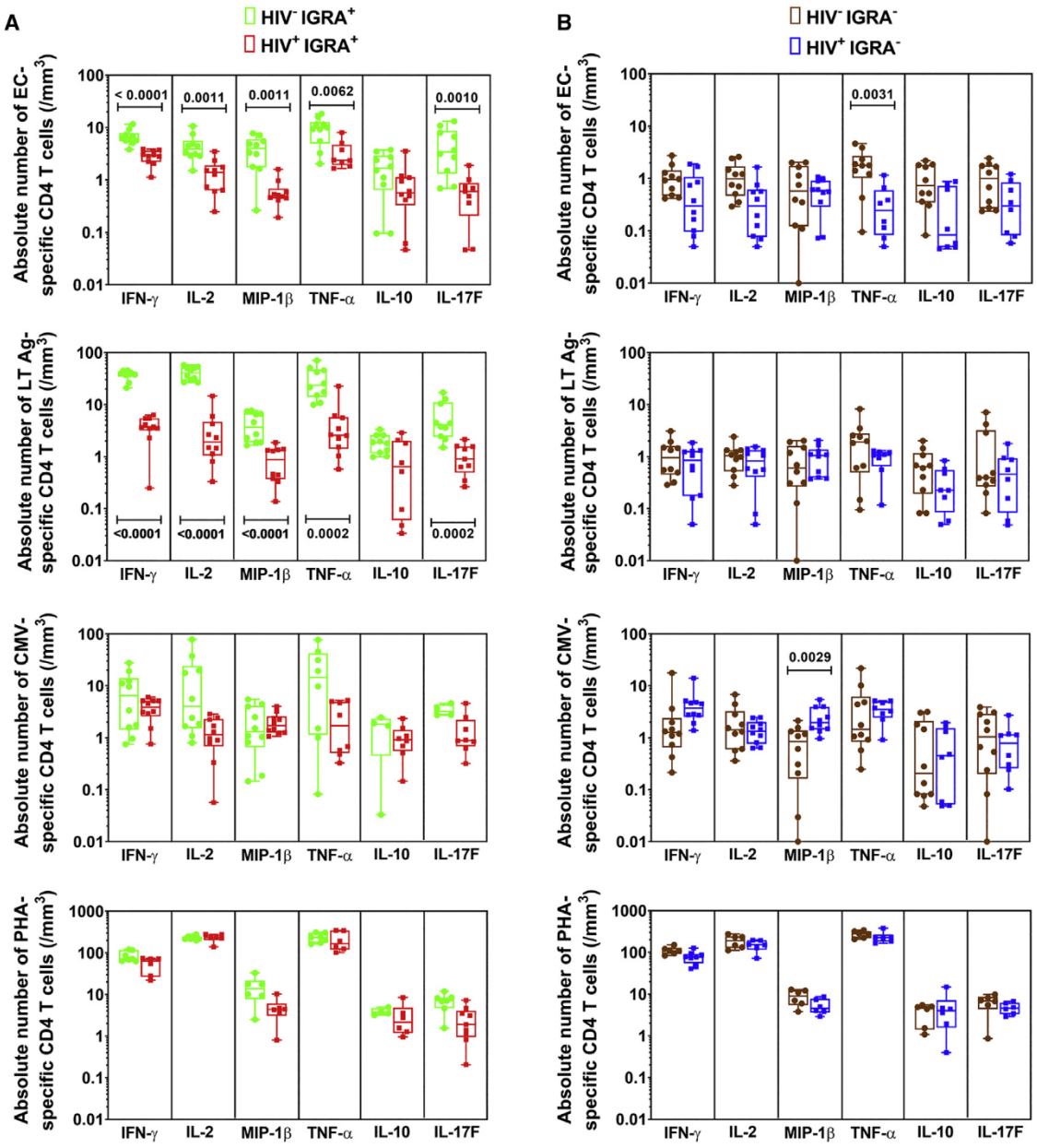

Figure 1. HIV Infection Impairs the Expression of Effector Cytokines in Mtb-Specific CD4⁺ T Cells

(A and B) PBMCs from (A) HIV⁻IGRA⁺ (n = 10, green) versus HIV⁺IGRA⁺ (n = 10, red) and (B) HIV⁻IGRA⁻ (n = 10, brown) versus HIV⁺IGRA⁻ (n = 10, blue) subjects were stimulated overnight with EC (10 μg/mL), LT Ag (10 μg/mL), CMVpp65 (1.7 μg/mL), and PHA (1 μg/mL). All HIV⁺ subjects were initiated on ART after collection of blood at baseline post diagnosis. CD3⁺CD4⁺ T cells were analyzed for intracellular expression of IFN-γ, IL-2, MIP-1β, TNF-α, IL-10, and IL-17F in a standard intracellular cytokine staining (ICS) assay. Frequencies of cytokine-producing total CD4⁺ T cells were obtained after background subtraction of values from its unstimulated control. Absolute numbers of antigen-specific CD4⁺ T cells were calculated by multiplying the frequencies of cytokine-positive CD4⁺ T cells by the total CD4 T cell count. Box-and-whisker plots show the inter-quartile range, and horizontal bars represent the median absolute numbers of total cytokine-positive CD4⁺ T cells. Statistical analysis was performed by Mann-Whitney two-tailed t test with Bonferroni's correction for multiple comparisons. $P < 0.05$ was considered statistically significant.

Arroyo et al., 2016) and can be impaired by HIV infection (Day et al., 2017; Diedrich and Flynn, 2011). We therefore evaluated the differences in polyfunctional CD4⁺ T cell responses between HIV⁻IGRA⁺ and HIV⁺IGRA⁺ subjects using a panel of eight key effector cytokines: IFN-γ, IL-2, TNF-α, MIP-1β, IL-10, IL-17A, IL-17F, and IL-22. Polyfunctionality was determined by analyzing all 256 different combinations of these eight cytokines stratified using the Boolean gating strategy in FlowJo and using combinatorial polyfunctionality analysis of antigen-specific T cell subsets (COMPASS) (Lin et al., 2015), an advanced bioinformatics

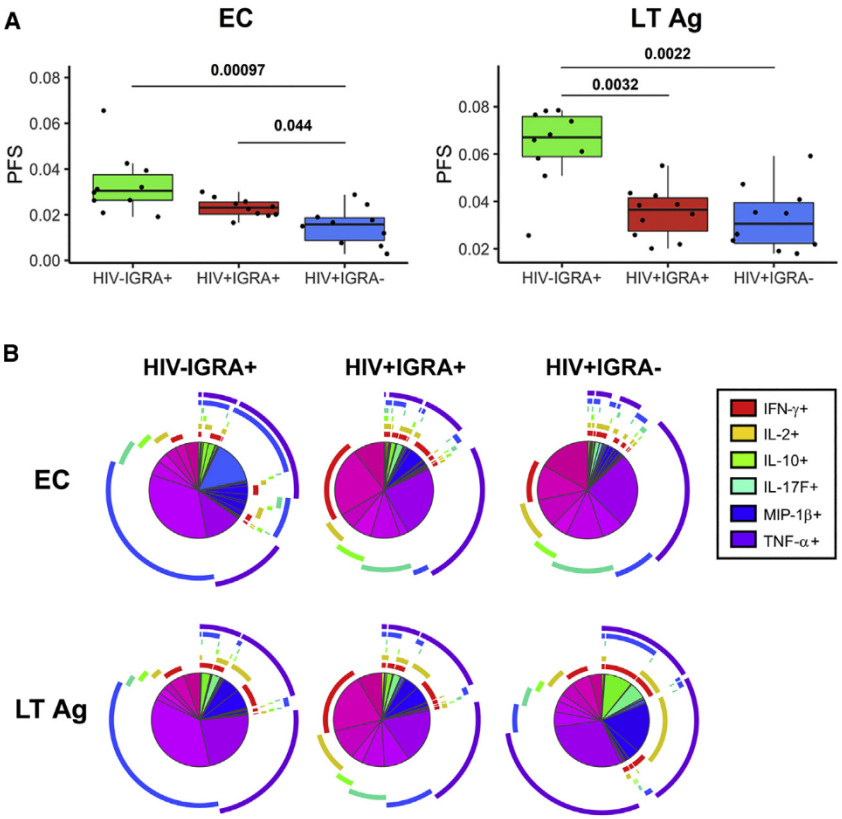

Figure 2. COMPASS and SPICE Analyses Reveal HIV Infection Reduces CD4$^+$ Polyfunctional Responses to EC and LT Ag in IGRA$^+$ and IGRA$^-$ Subjects

(A and B) PBMCs were stimulated overnight with EC and LT Ag, and CD3$^+$CD4$^+$ T cells were analyzed for intracellular expression of IFN-γ, IL-2, MIP-1β, TNF-α, IL-10, and IL-17F in a standard ICS assay. All HIV$^+$ subjects were initiated on ART after collection of blood at baseline post diagnosis. Boolean gates were created from the individual cytokine (listed above) in FlowJo to divide responding cells into 64 distinct subsets corresponding to all possible combinations of these functions, and the data were analyzed using COMPASS and SPICE software. (A) Boxplots show Mtb-specific CD4$^+$ T cell polyfunctionality scores (PFSs) analyzed by COMPASS in HIV$^-$IGRA$^+$ (green), HIV$^+$IGRA$^+$ (red), and HIV$^+$IGRA$^-$ (blue). For each antigen, pairwise differences between HIV$^-$IGRA$^+$ and other groups were based on a group-wise linear model fit to the PFS (null: $\beta_{group} - \beta_{HIV^-IGRA^+} = 0$ two-sided test), and p values were adjusted for multiple testing (see STAR Methods). (B) SPICE analyses for in-depth phenotypic profiling of Mtb-specific CD4$^+$ T cells in HIV$^-$IGRA$^+$ (n = 10), HIV$^+$IGRA$^-$ (n = 10), and HIV$^+$IGRA$^+$ (n = 10) subjects. Each slice of the pie corresponds to a distinct combination of six cytokines (IFN-γ, IL-2, TNF-α, IL-17F, IL-10, and MIP-1β) produced in response to EC and LT Ag stimulation. The pie charts depict the mean frequency for each of the 64 possible phenotypic profiles of Mtb-specific CD4$^+$ T cells. The arcs surrounding the pie charts indicate the proportion of the responses contributed by each of the single cytokines. A key to the colors used for different cytokines in the pie chart arcs is shown. $P < 0.05$ was considered statistically significant.

software to derive polyfunctionality scores (PFSs) (Figure 2A). Differences in PFSs between groups were estimated through a linear model fit to the PFS for each antigen (see STAR Methods). After multiple testing adjustments, significant reduction was observed in the CD4$^+$ T cell polyfunctional response to LT Ag stimulation and a trend for EC in HIV$^+$IGRA$^+$ compared with that of HIV$^-$IGRA$^+$ subjects (Figure 2A). Furthermore, consistent with the total cytokine data in Figure 1, the polyfunctional response in IGRA$^-$ subjects was significantly lower than that of IGRA$^+$ subjects.

COMPASS analysis was performed for in-depth visualization of CD4$^+$ T cell subsets simultaneously expressing one, two, three, four, and five combinations of cytokines in all subjects from three clinical groups (HIV$^-$IGRA$^+$, HIV$^+$IGRA$^+$, and HIV$^-$IGRA$^-$) in response to EC and LT Ag stimulation that are illustrated as heatmaps in Figure S5. We observed that single-positive cells expressing IFN-γ, TNF-α, and Th17 (IL-17A, IL-17F, and IL-22) cytokines mostly remained unchanged, with an increase only in IL-2$^+$ cells; however, MIP-1β and IL-10 single-positive cells were drastically reduced in HIV$^+$IGRA$^+$ compared with HIV$^-$IGRA$^+$ subjects in response to EC stimulation. CD4$^+$ subsets expressing TNF-α in combination with IL-2, MIP-1β, IL-10, or IL-22 as well as IL-10$^+$IL-17F$^+$ were markedly reduced in HIV$^+$IGRA$^+$ versus HIV$^-$IGRA$^+$ subjects. We also observed a slight decrease of 4$^+$ (IFN-γ$^+$IL-2$^+$TNF-α$^+$MIP-1β$^+$) CD4$^+$ T cell subset; however, no significant changes were observed in the probability of 3$^+$ subset (IFN-γ$^+$IL-2$^+$TNF-α$^+$) between the HIV$^-$IGRA$^+$ and HIV$^+$IGRA$^+$ subjects (Figure S5). Interestingly, there was a profound impairment in the polyfunctional response to LT Ag stimulation compared with EC, with HIV-infected IGRA$^+$ subjects having a relatively smaller proportion of cells that express a combination of two, three, four, and five cytokines compared with HIV-uninfected IGRA$^+$ subjects. The analysis also revealed IFN-γ$^+$IL-2$^+$ as well as dual subsets producing MIP-1β or IL-10 in combination with Th17 cytokines to be most significantly reduced. Within subsets that expressed three, four, or five cytokines, HIV infection considerably decreased subsets that predominantly expressed TNF-α and/or Th17 cytokines in combination with IL-10, although the probability of IFN-γ$^+$IL-2$^+$TNF-α$^+$ subset remained unchanged. No significant differences between HIV-infected and HIV-uninfected individuals were detected in the proportions of single-positive CD4$^+$ T cells except for IL-10$^+$ and MIP-1β$^+$ (Figure S5).

The polyfunctional CD4$^+$ T cell response was further probed by analysis of the above-mentioned data (Figure 2A) in simplified presentation of incredibly complex evaluation (SPICE) software (Roederer et al., 2011). Using this software, the global cytokine

profile induced in IGRA$^+$ subjects to EC and LT Ag stimulation represented as pie charts in Figure 2B was functionally similar, but each of these responses were profoundly impacted by HIV infection (Figure 2B). This analysis clearly demonstrates the striking loss of single MIP-1β^+ cells (shown as blue arcs) and the EC-specific double-positive TNF-α^+MIP-1β^+ subset but an increase of single TNF-α^+ cells (shown as purple arcs) in all HIV$^+$ subjects independent of IGRA status (Figure 2B). In addition, this analysis revealed that HIV reduces many combinations of 2^+, 3^+, 4^+, and 5^+ cells, while preserving single-positive IFN-γ, IL-2, IL-17F, and IL-10 cells in HIV$^+$IGRA$^+$ and HIV$^+$IGRA$^-$ compared with HIV$^-$IGRA$^+$ subjects, thereby indicating an overall impairment of polyfunctional responses in HIV$^+$ subjects (Figure 2B). Taken together, our data demonstrate that CD4$^+$ T cell polyfunctional responses are markedly impaired in HIV$^+$IGRA$^+$ subjects, with LT Ag-specific cells being particularly impacted.

HIV Infection Skews the Balanced Mtb-Specific Th17 Response in IGRA$^+$ Subjects

Previously, we have shown a balanced Mtb-specific Th17 response comprising both IL-17$^+$IFN-γ^+ pro-inflammatory and IL-17$^+$IL-10$^+$ anti-inflammatory effectors to be a hallmark of HIV$^-$IGRA$^+$ individuals (Rakshit et al., 2017). Therefore, we sought to evaluate the status of the Th17 response in IGRA$^+$ subjects following HIV infection. Using COMPASS, we conducted a detailed analysis of the probability of EC and LT Ag-specific CD4$^+$ Th17 cells for each subject averaged across selected functional profiles for either IFN-γ or IL-10 together with all combinations of IL-17A, IL-17F, and IL-22 (Figure 3A). HIV$^+$IGRA$^+$ and HIV$^+$IGRA$^-$ subjects had significantly fewer LT Ag-specific regulatory CD4$^+$ Th17 subsets co-expressing IL-10 with IL-17A/IL-17F/IL-22, whereas the reduction of these subsets was not statistically significant for EC-specific cells, indicating that the LT Ag-specific Th17 response was more significantly impacted by HIV infection compared with the EC response (Figure 3A).

To further interrogate the above-mentioned data, we used SPICE to identify the precise Mtb-specific Th17 subsets that were altered by HIV infection by separately enumerating the absolute numbers of three combinations of double-positive pro-inflammatory (IFN-γ^+IL-17A$^+$, IFN-γ^+IL-17F$^+$, and IFN-γ^+IL-22$^+$) and three combinations of double-positive anti-inflammatory or regulatory (IL-10$^+$IL-17A$^+$, IL-10$^+$IL-17F$^+$, and IL-10$^+$IL-22$^+$) Th17 cell subsets (see STAR Methods), with representative FACS profiles shown in Figure S6A. In Figure 3B, we demonstrate the impact of HIV infection on each of these six subsets in IGRA$^+$ subjects. We highlight the following salient points: (1) Absolute CD4$^+$ T cell numbers of all three EC- and LT Ag-specific regulatory Th17 subsets co-expressing IL-10, which form a minor but distinct viable cell population as confirmed by backgating analysis (Figure S6B), is significantly lower in HIV$^+$IGRA$^+$ than HIV$^-$IGRA$^+$ subjects (Figure 3B). (2) Although IFN-γ^+IL-17A$^+$ and IFN-γ^+IL-22$^+$ subsets were significantly reduced by HIV infection noticeably to LT Ag, but not to EC, stimulation, the absolute numbers of these pro-inflammatory subsets were relatively higher than the IL-10$^+$ regulatory subsets, suggesting that regulatory subsets are impacted to a greater extent upon HIV infection (Figure 3B).

Next, we conducted a detailed analysis of HIV infection on Mtb-specific Th17 subsets across seven different clinical groups where Th17 cells were grouped into pro-inflammatory (IFN-γ expression with either IL-17A/IL-17F or IL-22) or anti-inflammatory (IL-10 expression with either IL-17A/IL-17F or IL-22) subsets. In addition, we probed the impact of HIV infection on IFN-γ^+IL-10$^+$ cells, another anti-inflammatory regulatory subset (referred to as Tr1 cells) reportedly expanded in chronic infections, including TB (Trinchieri, 2001). Figure 3C shows the comparison of the three subsets (pro-inflammatory Th17 and anti-inflammatory/regulatory Th17 and Tr1) in IGRA$^+$ and IGRA$^-$ HIV$^+$ progressors; IGRA$^+$ HIV$^+$ LTNPs; HIV$^+$ subjects with TB and HIV uninfected IGRA$^+$, IGRA$^-$, and TB$^+$ subjects serving as controls. Absolute numbers of cytokine-positive cells corrected for multiple comparisons across these seven clinical groups are shown in Figure 3C, with salient observations as follows: (1) Most HIV$^-$IGRA$^-$ subjects (brown) lacked EC- and LT Ag-specific pro-inflammatory IFN-γ^+ Th17 cells but had low absolute numbers (less than 0.1%) of IL-10$^+$ regulatory Th17 cells. (2) Notably, HIV infection of IGRA$^-$ subjects enhanced the pro-inflammatory Th17 subset (blue). (3) Compared with HIV$^-$IGRA$^-$ subjects, HIV$^-$IGRA$^+$ subjects (green) had a greater LT Ag- and EC-specific Th17 response (0.1% and greater), with HIV infection inducing dramatic loss of regulatory IL-10$^+$ Th17 subsets (red). (4) A comparison of IGRA$^+$ HIV$^+$ progressors who had low CD4 T cell counts with those of IGRA$^+$ HIV$^+$ LTNPs with preserved CD4 T cell counts showed that LTNPs have mainly regulatory Th17 subsets with a low proportion of pro-inflammatory IFN-γ^+ Th17 subsets (magenta). (5) The data also highlight that HIV$^-$ subjects with TB (black) have the highest numbers of pro-inflammatory IFN-γ^+ Th17 cells compared with any other group with few regulatory IL-10$^+$IL-17$^+$ cells; however, HIV infection in TB$^+$ subjects leads to a further decrease in both regulatory as well as pro-inflammatory Th17 subsets (dark gray). (6) Furthermore, we demonstrate that IFN-γ^+IL-10$^+$ cells are present in HIV$^-$IGRA$^+$ and HIV$^+$IGRA$^+$ LTNP subjects but low in HIV$^+$IGRA$^+$ and HIV$^+$TB$^+$ groups. Taken together, these data provide strong evidence that HIV infection significantly impacts the balance between pro- and anti-inflammatory Mtb-specific Th17 subsets, with significant dysregulation of the Mtb-specific regulatory Th17 cells co-expressing IL-10 following chronic HIV infection of IGRA$^+$ subjects.

ART and ATT Therapies Enhance Mtb-Specific Total Cytokine Effector Responses

ART and ATT have been shown to increase the absolute numbers of Mtb-specific CD4$^+$ T cells in HIV$^-$IGRA$^+$ subjects (Chiacchio et al., 2018). We sought to investigate whether ART and ATT can restore Mtb-specific cytokine responses impacted by HIV and Mtb infection, respectively, through a longitudinal analysis of samples taken pre- and 1-year post treatment. ART increased the CD4 T cell count in all IGRA$^+$ subjects tested (Table S1). In addition, the absolute numbers of total LT Ag- and EC-specific IL-2, IL-10, IL-17F, and MIP-1β, but not IFN-γ and TNF-α, CD4$^+$ T cells were significantly enhanced by ART (Figure 4A). ATT treatment of HIV-uninfected subjects with TB also highlighted significant enhancement of IL-10$^+$ LT

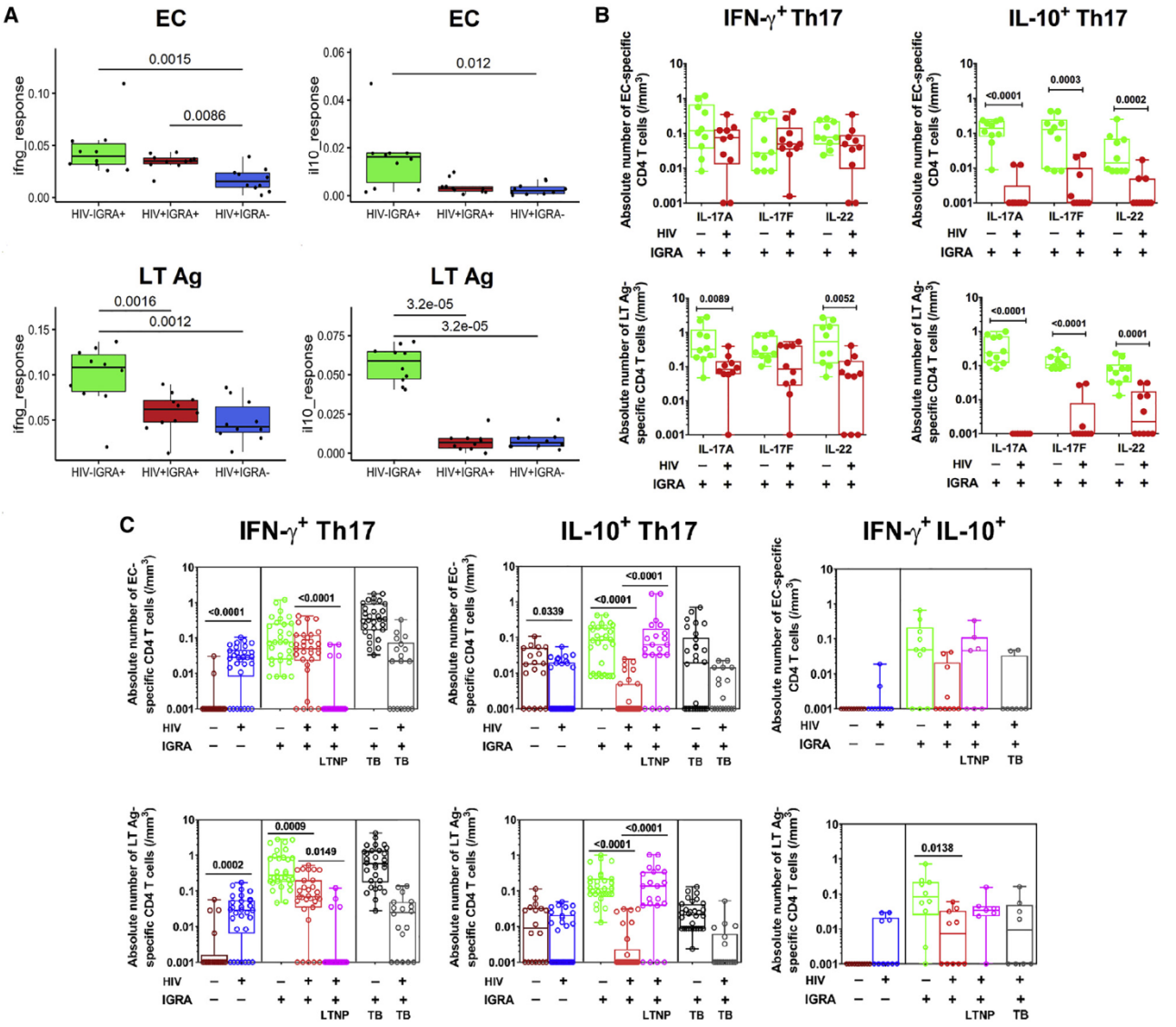

Figure 3. HIV Infection Leads to Skewing of Th17 Response in HIV$^+$IGRA$^+$ Chronic Progressors, but Not in Long-Term Non-progressors

(A–C) PBMCs were cultured overnight in the presence or absence of EC and LT Ag. CD3$^+$CD4$^+$ T cells were analyzed for intracellular expression of IFN-γ, IL-17A, IL-17F, IL-22, and IL-10. Boolean gates were created from the individual cytokine (listed above) in FlowJo to divide responding cells into 256 distinct subsets corresponding to all possible combinations of these functions, and the data were analyzed using COMPASS and SPICE software. All HIV$^+$ subjects were initiated on ART after collection of blood at baseline post diagnosis. (A) Boxplots of data analyzed in COMPASS are shown for the HIV$^-$IGRA$^+$ (n = 10, green), HIV$^+$IGRA$^+$ (n = 10, red), and HIV$^+$IGRA$^-$ (n = 10, blue) groups of probability scores of antigen-specific response for each subject, averaged across selected functional profiles (either IFN-γ$^+$ or IL-10$^+$ cells together with all combinations of IL-17A, IL-17F, and IL-22) and across EC or for LT Ag. Probabilities are derived from a COMPASS model fit to ICS data using the Th17 panel. A p value is shown tested for a difference between groups (two-sided t test). (B) HIV$^-$IGRA$^+$ (n = 10, green) and HIV$^+$IGRA$^+$ (n = 10, red) subjects were chosen for comparison of the individual Th17 pro-inflammatory (IFN-γ$^+$IL-17A$^+$, IFN-γ$^+$IL-17F$^+$, IFN-γ$^+$IL-22$^+$) or regulatory (IL-10$^+$IL-17A$^+$, IL-10$^+$IL-17F$^+$, IL-10$^+$IL-22$^+$) subsets and in (C) HIV$^-$IGRA$^-$ (n = 10, brown), HIV$^-$IGRA$^+$ (n= 10, green), HIV$^+$IGRA$^-$ (n = 10, blue), HIV$^+$IGRA$^+$ (n = 10, red), HIV$^+$IGRA$^+$LTNP (n = 7, magenta), HIV$^-$TB$^+$ (n = 10, black), and HIV$^+$TB$^+$ (n = 8, dark gray) subjects were compared for combined double-positive Th17 pro-inflammatory (IFN-γ with IL-17A/IL-17F/IL-22) or regulatory (IL-10 with IL-17A/IL-17F/IL-22) subsets and Tr1 cells (IFN-γ$^+$IL10$^+$) in response to EC or LT Ag pool stimulation. Box-and-whisker plots analyzed by SPICE show the inter-quartile range in absolute numbers, with horizontal bar representing the median of (B) individual or (C) combined cellular subsets. Statistical analysis was performed using a one-way ANOVA nonparametric Kruskal-Wallis test and corrected by Dunn's test for multiple comparisons. P < 0.05 was considered statistically significant.

Ag- and EC-specific and MIP-1β$^+$ LT Ag-specific CD4$^+$ T cells; all other effectors were not altered (Figure 4B). Therefore, ART treatment of HIV$^+$IGRA$^+$ subjects enhanced a broad range of total Mtb-specific T cell effectors, while ATT treatment led to partial restoration of cytokine responses in HIV-uninfected subjects with TB. Notably, ATT treatment of IGRA$^+$ subjects could not be conducted as ATT is only given to subjects with full-blown TB in India.

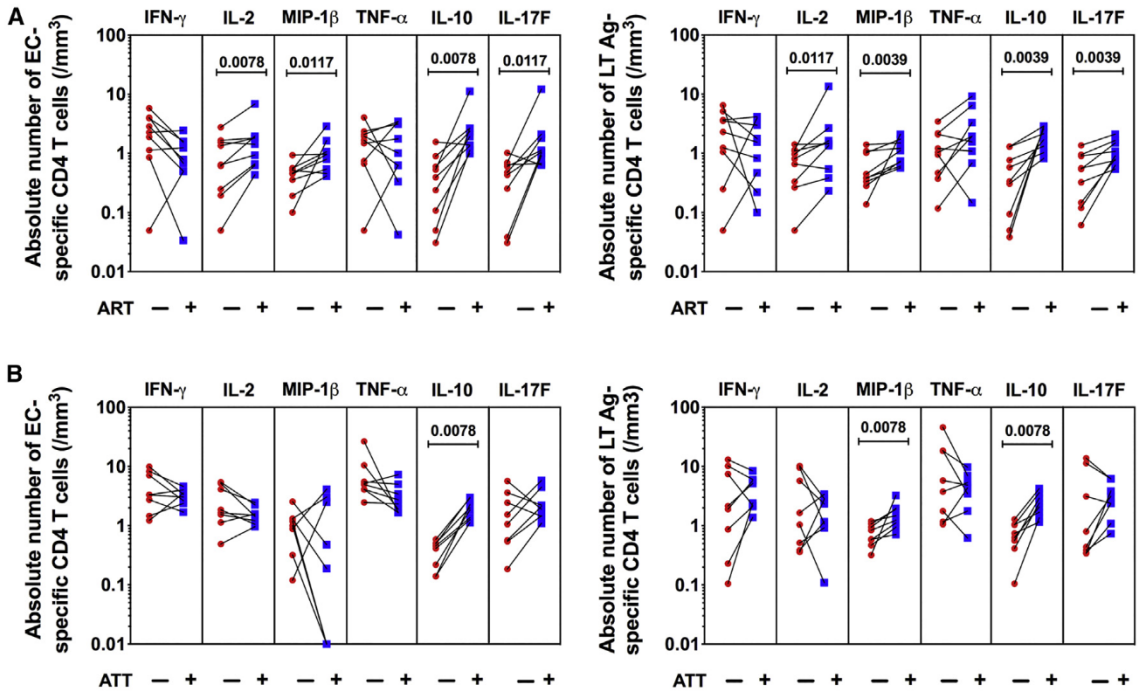

Figure 4. ART and ATT modulate CD4+ T effector cytokine responses in HIV$^+$ and TB$^+$ patients

(A and B) (A) PBMCs from HIV$^+$IGRA$^-$ and HIV$^+$IGRA$^+$ (n = 9) patients before ($^-$ART in red) and after ($^+$ART in blue) treatment were stimulated overnight with EC and LT Ag. (B) PBMCs from HIV-TB$^+$ (n = 8) patients before ($^-$ATT in red) and after ($^+$ATT in blue) treatment were stimulated overnight with EC and LT Ag. In both (A) and (B), CD3$^+$CD4$^+$ T cells were analyzed for intracellular expression of IFN-γ, IL-2, MIP-1β, TNF-α, IL-10, and IL-17F in a standard ICS assay. Dots connected with full lines represent matched pairs of patients post treatment ($^+$ART or $^+$ATT) with treatment naive controls ($^-$ART or $^-$ATT). Horizontal capped lines represent statistical comparisons between matched patients. Statistical analysis was performed by Wilcoxon matched-pairs signed rank-sum test with post hoc Bonferroni's correction for multiple comparisons. $P < 0.05$ was considered statistically significant.

ART and ATT Restore Regulatory Th17 Responses in HIV$^+$ and TB Patients

We next examined whether ART can specifically restore the skewed Mtb-specific Th17 response induced by HIV infection and whether ATT can restore these responses in TB-treated patients. We observed that ART significantly reduced the absolute numbers of pro-inflammatory IFN-γ$^+$ Th17 subsets and conversely increased regulatory IL-10$^+$ Th17 subsets in response to both EC and LT Ag stimulation (Figure 5A). ATT also significantly enhanced absolute numbers of LT Ag-specific IL-10$^+$IL-17A$^+$, IL-10$^+$IL-17F$^+$, and IL-10$^+$IL-22$^+$ subsets and EC-specific IL-10$^+$IL-17F$^+$ Th17 subsets; conversely, a trend was noted for ATT treatment to suppress EC-specific IL-17F and IL-22, but not IL-17A, cells that co-expressed IFN-γ (Figure 5B). In conclusion, both ART and ATT have the potential to restore the Mtb-specific regulatory Th17 response, with ART also effective in dampening the Mtb-specific pro-inflammatory Th17 response in HIV-infected IGRA$^+$ subjects.

Loss of Mtb-Specific Effector Cells in HIV-Infected IGRA$^+$ Subjects Is Not Due to Selective HIV Infection Associated with Reduced Expression of the Anti-HIV Chemokine MIP-1β

We next assessed whether the selective early loss of Mtb-specific effectors in HIV$^+$IGRA$^+$ subjects, as shown in Figure 1, was due to higher HIV infection levels and associated absence of anti-HIV chemokine MIP-1β expression by probing the viral load of antigen-specific CD4$^+$ T cells that expressed high (CMV-specific) versus low (Mtb-specific) levels of MIP-1β. Notably, all HIV$^+$ subjects with chronic HIV infection recruited to this study went on to subsequent ART treatment due to a declining CD4 T cell count. An overview protocol used to capture antigen-specific cells for analysis of viral load and cytokines is shown in Figure 6A. We used antigen-induced expression of CD154 and CD69 to capture specific cells as reported previously (Bacher and Scheffold, 2013). Both CD154$^+$CD69$^+$ (antigen-specific activated) and CD154$^-$CD69$^-$ (un-activated control) memory (CD45RA$^-$) CD4 T cells were captured by flow-cytometry-based cell sorting after stimulation of peripheral blood mononuclear cells (PBMCs) with Mtb antigens (EC or LT Ag) or with HIV-PTE (Env and Gag) or with CMVpp65 peptides. To verify the capture and stimulation efficacy, we first confirmed by qRT-PCR that the antigen-activated subsets in each case expressed higher levels of IL-2 and IFN-γ, key cytokines induced by T cell activation. For each antigen stimulation, we demonstrate that the CD154$^+$CD69$^+$ subset expressed significantly higher IFN-γ and IL-2 mRNA than the CD154$^-$CD69$^-$ counterpart (Figures 6B and 6C). We also demonstrate that Mtb-specific CD154$^+$CD69$^+$ cells do not express higher MIP-1β than their CD154$^-$CD69$^-$ counterpart, whereas CMV-specific cells did (Figure 6D). This qRT-PCR data complement the data in Figure 1 and confirm the captured

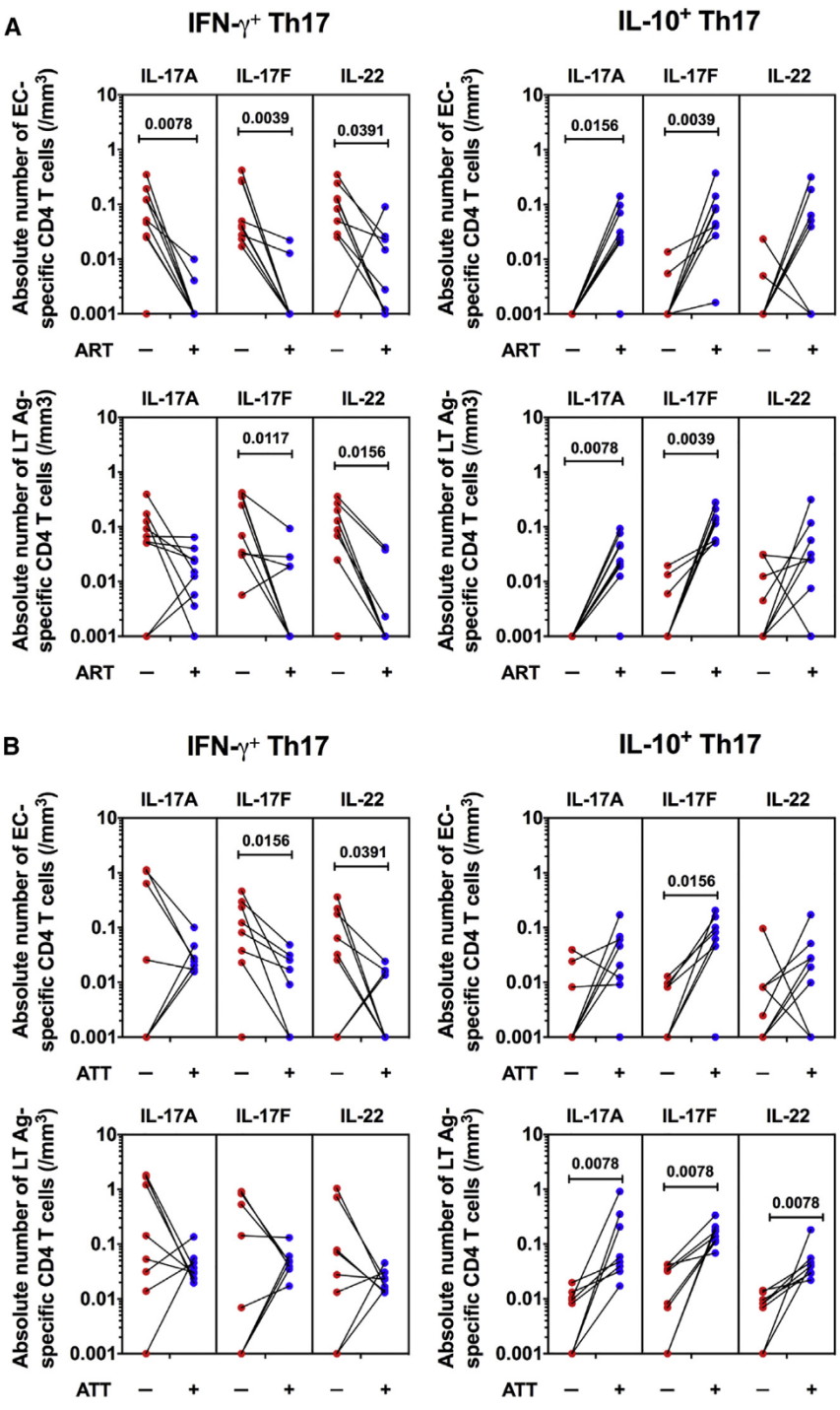

Figure 5. ART and ATT Restore Regulatory Th17 Response in HIV-Infected and Active TB Patients

(A and B) (A) PBMCs from HIV$^+$ subjects (n = 9) before (−ART, red) and after 1 year (+ART, blue) of treatment were cultured overnight in the presence or absence of EC and LT Ag. (B) PBMCs from HIV-TB$^+$ patients (n = 8) before (−ATT, red) and after 6 months (+ATT, blue) of treatment were cultured overnight in the presence or absence of EC and LT Ag. In both (A) and (B), CD3$^+$CD4$^+$ T cells were analyzed for expression of IL-17A, IL-17F, and IL-22 in combination with IFN-γ or IL-10 using SPICE. Dots connected with full lines represent matched pairs of patients post treatment with treatment-naive controls. Horizontal capped lines represent statistical comparisons between matched patients. Statistical analysis was performed using the Wilcoxon matched-pairs signed rank-sum test with post hoc Bonferroni's correction for multiple comparisons. $P < 0.05$ was considered statistically significant.

Mtb-specific cells to be MIP-1β^{low} relative to the captured CMV-specific cells.

To quantify HIV DNA copy number, a standard curve was first optimized to detect as low as one copy of CD3 (reference gene) and HIV-1 LTR (Figure S7); the qPCR assay was sensitive for six copies of CD3 gene and three copies of HIV-1 LTR gene, with 100% confidence as determined by testing genomic DNA isolated from ACH2 cells. After cutoff to exclude non-specific signals from low HIV-1 DNA loads (cutoff HIV-1 LTR gene qRT-PCR signal Ct = 30) and correlation of cell counts, the HIV-1 DNA copy number did not significantly vary in CD154$^+$CD69$^+$ T cells across different antigen specificities (Figure 6E). Antigen stimulation in the absence of ART for 16 h is recognized to be a weak stimulus for new HIV DNA synthesis; consistent with this, we show no significant difference in HIV DNA load between the CD154$^+$CD69$^+$ and the CD154$^-$CD69$^-$ counterpart in Mtb- and HIV-specific cells; however, there was a weak induction of HIV DNA in CMV-stimulated cells (Figure 6F).

Cell-associated HIV RNA was simultaneously quantified in each population by calculating the fold change (FC) of Gag gene expression in the CD154$^+$CD69$^+$ and the CD154$^-$CD69$^-$ counterpart relative to a negative control cell culture not exposed to any antigen. There was no significant difference in HIV RNA levels between CD154$^+$CD69$^+$ cells of different antigen specificities (Figure 6G). In addition, the HIV RNA levels in CD154$^+$CD69$^+$ versus CD154$^-$CD69$^-$ cells did not differ significantly, indicating no new burst of HIV Gag DNA translation following antigen stimulation (Figure 6H). We can confirm that this lack of induction of cell associated HIV RNA and HIV DNA at 16 h post antigen stimulation was not due to inefficient activation as all antigens significantly induced IFN-γ and IL-2 in the CD154$^+$CD69$^+$ compared with the CD154$^-$CD69$^-$ counterpart (Figures 6B and 6C). Furthermore, consistent with previous data

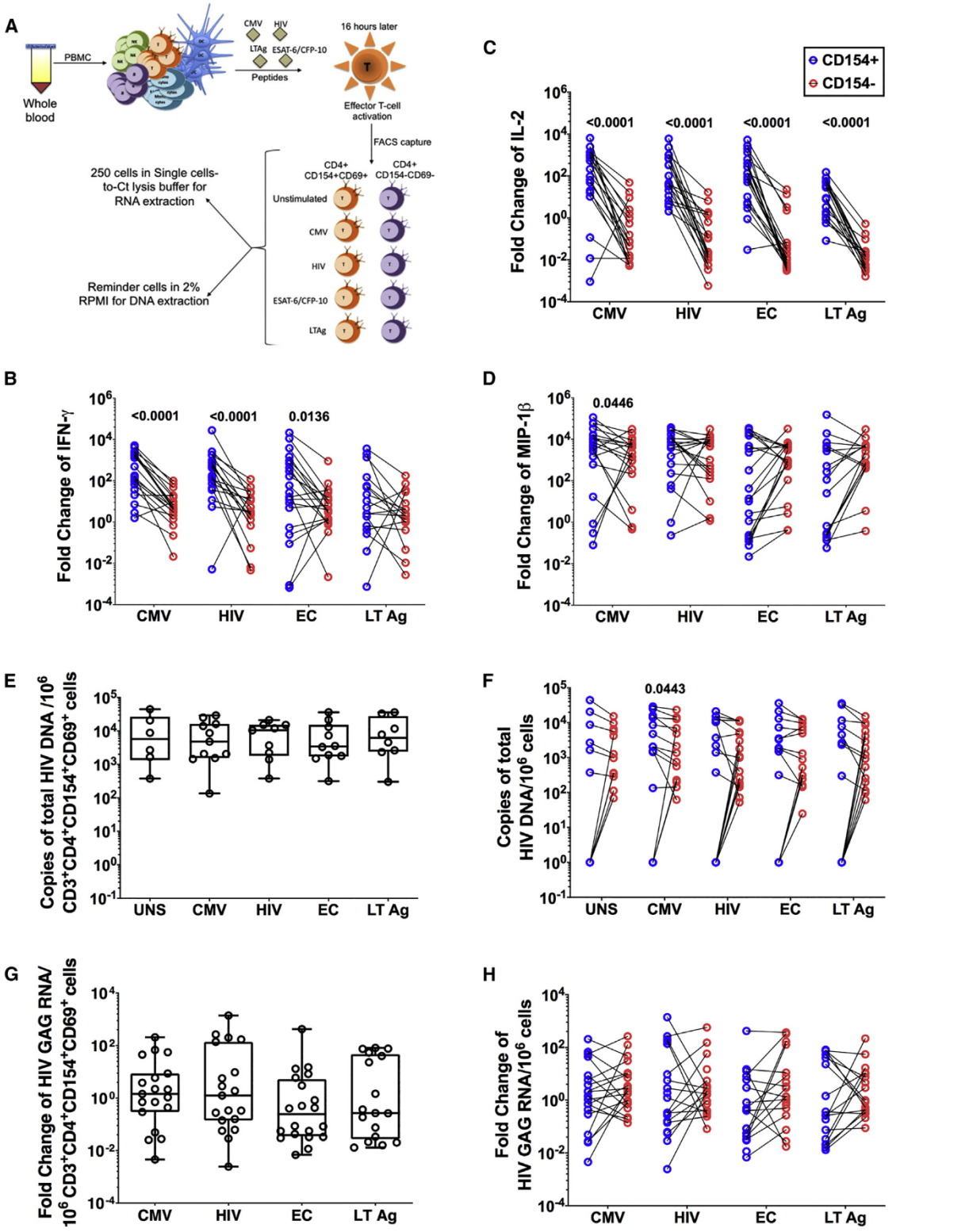

(legend on next page)

(Geldmacher et al., 2010), $CD4^+$ T cells stimulated with the HIV-PTE pool exhibited a higher proportion (41%) of cell-associated HIV RNA than Mtb- and CMV-specific cells or total memory cells. Therefore, we provide strong evidence that HIV does not exclusively infect MIP-$1\beta^{low}$ Mtb-specific cells from $IGRA^+$ subjects with chronic HIV infection since equivalent viral burden was detected in MIP-$1\beta^{hi}$ CMV-specific T cells from the same subjects. In summary, MIP-1β levels do not seem to govern *in vivo* HIV infection levels of antigen-specific $CD4^+$ T cell subsets in $IGRA^+$ subjects with chronic HIV infection.

DISCUSSION

This study provides fresh insights into the impact of HIV infection on the nature of the Mtb-specific $CD4^+$ T cell response, particularly the Th17 response, and unravels probable mechanisms that underpin why HIV infection is known to predispose $IGRA^+$ subjects to active TB, a topic of recognized global health importance. The increased vulnerability of Mtb-specific $CD4^+$ T cells to HIV infection due to low MIP-1β expression is an attractive hypothesis for explaining why HIV selectively reduces the frequencies of Mtb-specific MIP-$1\beta^{low}$ effectors, while preserving MIP-$1\beta^{hi}$ CMV-specific $CD4^+$ T cell effectors (see Geldmacher et al., 2010). In keeping with previous data (Amelio et al., 2019; Diedrich and Flynn, 2011; Murray et al., 2018), we confirm that HIV infection of $IGRA^+$ subjects selectively impairs Mtb-specific $CD4^+$ T cell effectors expressing several key cytokines, including IFN-γ, IL-2, TNF-α, MIP-1β, IL-17, and IL-10, while preserving recall responses to CMV. Additionally, in this study we report that MIP-$1\beta^{low}$ Mtb-specific cells isolated from HIV-infected $IGRA^+$ subjects harbored similar viral load compared with MIP-$1\beta^{hi}$ CMV-specific cells. A critical explanation for this lack of concurrence between our viral load data and those of Geldmacher et al. (2010) may be linked to significant differences in the clinical stage of HIV-infected subjects studied. Geldmacher et al. (2010) measured viral load in Mtb- and CMV-specific cells isolated from $IGRA^+$ subjects in the acute phase of HIV infection, before persistent loss of peripheral CD4 T cell counts had occurred, whereas we studied $IGRA^+$ subjects with chronic HIV infection with significantly lower CD4 T cell counts than uninfected controls (see Table 1). We contend that in the scenario of rising viral load and declining $CD4^+$ counts, as in the case of patients we studied, MIP-1β expression in $CD4^+$ T cells is less critical in setting a threshold for HIV infection and instead may be driven by chronic T cell activation.

HIV-mediated functional impairment of Mtb-specific $CD4^+$ T cell immune responses may also contribute to erosion of anti-TB immunity and thereby predispose $IGRA^+$ subjects to TB (Esmail et al., 2018). Several studies have investigated the quality of Mtb-specific $CD4^+$ T cell response in the context of HIV infection and reported a steady deterioration in the polyfunctionality of $CD4^+$ T cells (Day et al., 2017; Murray et al., 2018). Likewise, we, too, observed significant impairment of the overall polyfunctional $CD4^+$ T cell response, especially to LT Ag in HIV^+IGRA^+ subjects, which was restored following ART. Beyond polyfunctionality, there is particular interest in understanding how HIV infection impacts Mtb-specific Th17 responses, given their increasing importance in anti-TB immunity (Rakshit et al., 2017, 2019; Dijkman et al., 2019). In this study, we have addressed this issue and provide the first evidence that HIV infection significantly reduces the frequency of Mtb-specific IL-10 and IL-17 co-expressing $CD4^+$ T cells in $IGRA^+$ subjects. Understanding how HIV infection induces loss of $IL\text{-}17^+IL\text{-}10^+$ is important. One mechanism may be linked to the efficient replication of HIV in Th17 cells in the gut (Bixler and Mattapallil, 2013). Gut-homing $CXCR3^+CCR6^+CD4^+$ Th1/Th17 cells with increased TNF-α/IL-10 ratio is reportedly highly permissive to HIV infection (Gosselin et al., 2010; Alvarez et al., 2013). Moreover, HIV is thought to preferentially replicate in naive precursors of regulatory Th17 cells that could possibly lead to distorted polarization of Th17 cells toward the pathogenic phenotype in the presence of inflammatory environment in the gut (DaFonseca et al., 2015). We therefore propose that by reducing the frequencies of anti-inflammatory $IL\text{-}10^+$Th17 cells while sparing pathogenic IFN-γ^+Th17 cells, HIV creates a niche for persistent replication. Furthermore, the nature of HIV infection clearly influences the changes induced in the Th17 response. Thus, LTNP subjects with a stable CD4 count in contrast to HIV^+IGRA^+ progressors, had a robust Mtb-specific Th17 response that included largely anti-inflammatory $IL\text{-}10^+IL\text{-}17^+$ cells and few pro-inflammatory IFN-$\gamma^+IL\text{-}17^+$ cells. ART treatment of chronic HIV-infected $IGRA^+$ progressors restored their Mtb-specific responses, including polyfunctional cells and $IL\text{-}10^+IL\text{-}17^+$ anti-inflammatory cells, thus confirming HIV infection to be a major driver of these immune changes.

Figure 6. Cell-Associated HIV DNA, HIV RNA, and Cytokine Production Are Enhanced in Activated $CD3^+CD4^+CD45RA^-CD154^+CD69^+$ Cells Compared with Un-activated $CD3^+CD4^+CD45RA^-CD154^-CD69^-$ Counterpart in HIV-Infected Subjects, but Do Not Significantly Vary among Cells of Different Antigen Specificities

(A) Schematic overview of flow-cytometry-based cell sorting of antigen-specific memory $CD4^+$ T cells for quantification of cell-associated HIV DNA, HIV RNA, and cytokines. PBMCs from HIV^+ $IGRA^-$ and $IGRA^+$ subjects were first blocked with 0.5 μg/mL CD40 (HB14) antibody for 15 min and then stimulated with anti-CD28/CD49d costimulatory antibody and antigen (EC, LT Ag, CMVpp65, and HIV-PTE [Env-1, -2, and -3 and Gag -1 and -2] pools) for 16 h. The next day, 100–250 effector cells were directly sorted for $CD3^+CD4^+CD45RA^-CD154^+CD69^+$ (activated) and $CD3^+CD4^+CD45RA^-CD154^-CD69^-$ (resting) populations into single cells in CT lysis buffer for RNA extraction (cytokine and HIV RNA), whereas the remainder of the cells were collected in 2% RPMI for HIV DNA extraction. Comparison of (B) IFN-γ, (C) IL-2, and (D) MIP-1β gene expression in sorted cells of different antigen specificities. The cDNA was pre-amplified for cytokine mRNA along with glyceraldehyde 3-phosphate dehydrogenase (GAPDH) (reference gene). The fold change of cytokine mRNA is shown in $CD154^+$ versus $CD154^-$ T cells, which indicates efficient activation of $CD3^+CD4^+CD45RA^-CD154^+CD69^+$ and not its bystander counterpart $CD3^+CD4^+CD45RA^-CD154^-CD69^-$ T cells by various antigens. (E) HIV DNA copy number was estimated in different Ag-specific $CD154^+CD69^+$ cells. (F) Comparison of HIV DNA copy number in $CD154^+CD69^+$ versus $CD154^-CD69^-$ cells stimulated with different antigens. (G) Comparative fold change of HIV Gag mRNA in antigen-stimulated $CD154^+CD69^+$ cells relative to its unstimulated control. (H) Comparison of HIV Gag mRNA $CD154^+CD69^+$ versus $CD154^+CD69^+$ cells upon stimulation with different antigens. Statistical analysis was performed using the Kruskal-Wallis test and Wilcoxon matched-pairs signed rank-sum test. $P < 0.05$ was considered statistically significant.

Additional key mechanisms by which HIV may alter the balance of IL-10$^+$ and IFN-γ^+ Th17 subsets may be linked to HIV-driven changes in cytokines that are known to drive Th17 cell differentiation. A combination of several factors involving lineage-specific polarizing cytokines such as IL-23, IL-1β as well as IL-2, CCR6, signaling mediators, transcription factors, metabolism, and glucocorticoids are known to act in synergy to regulate the Th17/Treg balance and inter-Th17 subset balance (Yang et al., 2016; Seki and Nishizawa, 2016). Interestingly in the context of TB, Th17 cells polarized under a hypoxic environment secrete IL-10 in the TB granuloma (Volchenkov et al., 2017). Moreover, the paucity of the phenotypically naive CD4$^+$ T cell subsets, nTregs, and CD25$^+$CD127$^+$FoxP3$^-$ enriched in Th17-lineage committed cells has been associated with greater permissiveness to abortive and/or integrative HIV infection and may be a potential mechanism contributing to Th17 deficiency in HIV-infected subjects (Gosselin et al., 2010). Taken together, limited expression of Th17-specific growth factors (e.g., IL-21, TGF-β) required for differentiation and maintenance of regulatory Th17 cells in the inflammatory scenario of the HIV-infected gut may contribute to the loss of Mtb-specific IL-17$^+$IL-10$^+$ cells in IGRA$^+$ subjects with chronic HIV infection.

To summarize, we provide first evidence that HIV infection disrupts the Mtb-specific Th17 response by dramatically reducing the frequency of IL-17$^+$ cells that co-express IL-10, a loss that is pathogen driven and can be restored by ART. In addition, our data indicate that HIV skews the Mtb-specific Th17 response toward a pro-inflammatory profile in chronic IGRA$^+$ progressors, a pathogenic signature that is characteristic of subjects with active TB, whereas the Mtb-specific regulatory Th17 response is retained in HIV-infected IGRA$^+$ LTNP. Further analysis of HIV infection in Th17 subsets is warranted. Interestingly, our results corroborate recent findings that show antibody-induced CD4$^+$ T cell depletion alone is insufficient to trigger the onset of TB in macaques with latent TB in the absence of HIV infection (Bucşan et al., 2019). Furthermore, chronically simian immunodeficiency virus (SIV)-infected macaques with latent Mtb infection that eventually progressed to TB displayed enhanced immune activation, inflammation, and distorted CD4$^+$ T cell differentiation phenotypes compared with macaques that did not progress to TB, even though both groups had undergone massive SIV-induced CD4$^+$ T cell depletion (Bucşan et al., 2019). Therefore, HIV-induced preferential loss of Mtb-specific IL-10$^+$ regulatory CD4$^+$ Th17 cells may be detrimental to the host because a balanced immune response is likely crucial for Mtb containment.

STAR★METHODS

Detailed methods are provided in the online version of this paper and include the following:

- KEY RESOURCES TABLE
- RESOURCE AVAILABILITY
  - Lead Contact
  - Materials Availability
  - Data and Code Availability
- EXPERIMENTAL MODEL AND SUBJECT DETAILS
  - Study population
  - HIV uninfected healthy IGRA$^+$ and IGRA$^-$ subjects
  - Pulmonary and Extrapulmonary TB
  - HIV$^+$progressors, LTNP and HIV-TB coinfected patients
  - Sample collection and processing
- METHOD DETAILS
  - Intracellular cytokine staining (ICS) assay and multiparameter flow cytometry
  - Flow cytometry and data analysis
  - COMPASS analysis of flow cytometry data
  - Capture of antigen-specific CD4$^+$ T cells
  - DNA isolation
  - Real-Time Quantitative Reverse Transcription PCR PCR (qRT-PCR) for quantification of total cell-associated HIV DNA
  - Linearity, specificity and sensitivity of qRT-PCR assay to quantify cell-associated HIV DNA
  - Relative quantification of cytokines and cell-associated HIV-1 RNA
- QUANTIFICATION AND STATISTICAL ANALYSIS

SUPPLEMENTAL INFORMATION

Supplemental Information can be found online at https://doi.org/10.1016/j.celrep.2020.108451.

ACKNOWLEDGMENTS

The authors thank the volunteers for participating in this study and acknowledge the contributions of clinical research workers at National Aids Research Institute and St. John's Research Institute. We also thank the central IISc Biosafety Level 3 facility for help with flow cytometry. This work was funded principally by a Centre of Excellence grant to A.V. from the Department of Biotechnology, Government of India (BT/PR10394/MED/29/1128/2016). We acknowledge additional funding for antigen synthesis by EC HORIZON2020, TBVAC2020, and EC FP7 EURIPRED (FP7-INFRA-2012 grant 312661) to A.V. and T.H.M.O.

AUTHOR CONTRIBUTIONS

S.R., N.H., S.V.A., and A.V. designed the study. S.R. performed the immunology experiments and analyzed flow cytometry data. N.H. and S.V.A. performed the DNA and RNA PCR experiments and analyzed the data. V.A. helped with sorting, acquisition, and data analysis. B.K.S. and P.N.S. helped with processing of blood from clinical cohorts. G.F. performed the main bioinformatic and immuno-informatic analyses. G.D., R.P., M.G., and M.T. were clinical investigators. A.J.U.K., C.D., and R.G.V. collected clinical samples; provided the patient details; and wrote the clinical methodology for the manuscript. T.H.M.O. supplied the latency antigen recombinant proteins. S.R., N.H., and S.V.A. wrote the manuscript. S.C.D.R., T.H.M.O., M.T., and A.V. edited the manuscript.

DECLARATION OF INTERESTS

The authors declare no competing interests.

Received: May 10, 2020
Revised: September 15, 2020
Accepted: November 9, 2020
Published: December 1, 2020

REFERENCES

Acosta-Rodriguez, E.V., Rivino, L., Geginat, J., Jarrossay, D., Gattorno, M., Lanzavecchia, A., Sallusto, F., and Napolitani, G. (2007). Surface phenotype and antigenic specificity of human interleukin 17-producing T helper memory cells. Nat. Immunol. *8*, 639–646.

Ahmed, A., Rakshit, S., and Vyakarnam, A. (2016). HIV-TB co-infection: mechanisms that drive reactivation of Mycobacterium tuberculosis in HIV infection. Oral Dis. *22* (*Suppl 1*), 53–60.

Alvarez, Y., Tuen, M., Shen, G., Nawaz, F., Arthos, J., Wolff, M.J., Poles, M.A., and Hioe, C.E. (2013). Preferential HIV infection of CCR6+ Th17 cells is associated with higher levels of virus receptor expression and lack of CCR5 ligands. J. Virol. *87*, 10843–10854.

Amelio, P., Portevin, D., Hella, J., Reither, K., Kamwela, L., Lweno, O., Tumbo, A., Geoffrey, L., Ohmiti, K., Ding, S., et al. (2019). HIV Infection Functionally Impairs Mycobacterium tuberculosis-Specific CD4 and CD8 T-Cell Responses. J. Virol. *93*, e01728, e18.

Arroyo, L., Rojas, M., Franken, K.L., Ottenhoff, T.H., and Barrera, L.F. (2016). Multifunctional T Cell Response to DosR and Rpf Antigens Is Associated with Protection in Long-Term Mycobacterium tuberculosis-Infected Individuals in Colombia. Clin. Vaccine Immunol. *23*, 813–824.

Auguste, P., Tsertsvadze, A., Pink, J., Court, R., McCarthy, N., Sutcliffe, P., and Clarke, A. (2017). Comparing interferon-gamma release assays with tuberculin skin test for identifying latent tuberculosis infection that progresses to active tuberculosis: systematic review and meta-analysis. BMC Infect. Dis. *17*, 200.

Bacher, P., and Scheffold, A. (2013). Flow-cytometric analysis of rare antigen-specific T cells. Cytometry A *83*, 692–701.

Bell, L.C.K., and Noursadeghi, M. (2018). Pathogenesis of HIV-1 and Mycobacterium tuberculosis co-infection. Nat. Rev. Microbiol. *16*, 80–90.

Bixler, S.L., and Mattapallil, J.J. (2013). Loss and dysregulation of Th17 cells during HIV infection. Clin. Dev. Immunol. *2013*, 852418.

Bronke, C., Palmer, N.M., Jansen, C.A., Westerlaken, G.H., Polstra, A.M., Reiss, P., Bakker, M., Miedema, F., Tesselaar, K., and van Baarle, D. (2005). Dynamics of cytomegalovirus (CMV)-specific T cells in HIV-1-infected individuals progressing to AIDS with CMV end-organ disease. J. Infect. Dis. *191*, 873–880.

Bucşan, A.N., Chatterjee, A., Singh, D.K., Foreman, T.W., Lee, T.H., Threeton, B., Kirkpatrick, M.G., Ahmed, M., Golden, N., Alvarez, X., et al. (2019). Mechanisms of reactivation of latent tuberculosis infection due to SIV coinfection. J. Clin. Invest. *129*, 5254–5260.

Caetano, D.G., de Paula, H.H.S., Bello, G., Hoagland, B., Villela, L.M., Grinsztejn, B., Veloso, V.G., Morgado, M.G., Guimarães, M.L., and Côrtes, F.H. (2020). HIV-1 elite controllers present a high frequency of activated regulatory T and Th17 cells. PLoS ONE *15*, e0228745.

Carpenter, C., Sidney, J., Kolla, R., Nayak, K., Tomiyama, H., Tomiyama, C., Padilla, O.A., Rozot, V., Ahamed, S.F., Ponte, C., et al. (2015). A side-by-side comparison of T cell reactivity to fifty-nine Mycobacterium tuberculosis antigens in diverse populations from five continents. Tuberculosis (Edinb.) *95*, 713–721.

Chiacchio, T., Petruccioli, E., Vanini, V., Cuzzi, G., La Manna, M.P., Orlando, V., Pinnetti, C., Sampaolesi, A., Antinori, A., Caccamo, N., and Goletti, D. (2018). Impact of antiretroviral and tuberculosis therapies on $CD4^+$ and $CD8^+$ HIV/M. tuberculosis-specific T-cell in co-infected subjects. Immunol. Lett. *198*, 33–43.

Ciccone, E.J., Greenwald, J.H., Lee, P.I., Biancotto, A., Read, S.W., Yao, M.A., Hodge, J.N., Thompson, W.L., Kovacs, S.B., Chairez, C.L., et al. (2011). CD4+ T cells, including Th17 and cycling subsets, are intact in the gut mucosa of HIV-1-infected long-term nonprogressors. J. Virol. *85*, 5880–5888.

Coppola, M., and Ottenhoff, T.H. (2018). Genome wide approaches discover novel Mycobacterium tuberculosis antigens as correlates of infection, disease, immunity and targets for vaccination. Semin. Immunol. *39*, 88–101.

DaFonseca, S., Niessl, J., Pouvreau, S., Wacleche, V.S., Gosselin, A., Cleret-Buhot, A., Bernard, N., Tremblay, C., Jenabian, M.A., Routy, J.P., and Ancuta, P. (2015). Impaired Th17 polarization of phenotypically naive CD4(+) T-cells during chronic HIV-1 infection and potential restoration with early ART. Retrovirology *12*, 38.

Day, C.L., Mkhwanazi, N., Reddy, S., Mncube, Z., van der Stok, M., Klenerman, P., and Walker, B.D. (2008). Detection of polyfunctional Mycobacterium tuberculosis-specific T cells and association with viral load in HIV-1-infected persons. J. Infect. Dis. *197*, 990–999.

Day, C.L., Abrahams, D.A., Harris, L.D., van Rooyen, M., Stone, L., de Kock, M., and Hanekom, W.A. (2017). HIV-1 Infection Is Associated with Depletion and Functional Impairment of *Mycobacterium tuberculosis*-Specific CD4 T Cells in Individuals with Latent Tuberculosis Infection. J. Immunol. *199*, 2069–2080.

Diedrich, C.R., and Flynn, J.L. (2011). HIV-1/mycobacterium tuberculosis coinfection immunology: how does HIV-1 exacerbate tuberculosis? Infect. Immun. *79*, 1407–1417.

Dijkman, K., Sombroek, C.C., Vervenne, R.A.W., Hofman, S.O., Boot, C., Remarque, E.J., Kocken, C.H.M., Ottenhoff, T.H.M., Kondova, I., Khayum, M.A., et al. (2019). Prevention of tuberculosis infection and disease by local BCG in repeatedly exposed rhesus macaques. Nat. Med. *25*, 255–262.

Douek, D.C., Picker, L.J., and Koup, R.A. (2003). T cell dynamics in HIV-1 infection. Annu. Rev. Immunol. *21*, 265–304.

Elhed, A., and Unutmaz, D. (2010). Th17 cells and HIV infection. Curr. Opin. HIV AIDS *5*, 146–150.

Esmail, H., Riou, C., Bruyn, E.D., Lai, R.P.J., Harley, Y.X.R., Meintjes, G., Wilkinson, K.A., and Wilkinson, R.J. (2018). The Immune Response to Mycobacterium tuberculosis in HIV-1-Coinfected Persons. Annu. Rev. Immunol. *36*, 603–638.

Foreman, T.W., Mehra, S., LoBato, D.N., Malek, A., Alvarez, X., Golden, N.A., Bucşan, A.N., Didier, P.J., Doyle-Meyers, L.A., Russell-Lodrigue, K.E., et al. (2016). CD4+ T-cell-independent mechanisms suppress reactivation of latent tuberculosis in a macaque model of HIV coinfection. Proc. Natl. Acad. Sci. USA *113*, E5636–E5644.

Franken, K.L., Hiemstra, H.S., van Meijgaarden, K.E., Subronto, Y., den Hartigh, J., Ottenhoff, T.H., and Drijfhout, J.W. (2000). Purification of his-tagged proteins by immobilized chelate affinity chromatography: the benefits from the use of organic solvent. Protein Expr. Purif. *18*, 95–99.

Frentsch, M., Arbach, O., Kirchhoff, D., Moewes, B., Worm, M., Rothe, M., Scheffold, A., and Thiel, A. (2005). Direct access to CD4+ T cells specific for defined antigens according to CD154 expression. Nat. Med. *11*, 1118–1124.

Geldmacher, C., and Koup, R.A. (2012). Pathogen-specific T cell depletion and reactivation of opportunistic pathogens in HIV infection. Trends Immunol. *33*, 207–214.

Geldmacher, C., Ngwenyama, N., Schuetz, A., Petrovas, C., Reither, K., Heeregrave, E.J., Casazza, J.P., Ambrozak, D.R., Louder, M., Ampofo, W., et al. (2010). Preferential infection and depletion of Mycobacterium tuberculosis-specific CD4 T cells after HIV-1 infection. J. Exp. Med. *207*, 2869–2881.

Gideon, H.P., Phuah, J., Myers, A.J., Bryson, B.D., Rodgers, M.A., Coleman, M.T., Maiello, P., Rutledge, T., Marino, S., Fortune, S.M., et al. (2015). Variability in tuberculosis granuloma T cell responses exists, but a balance of pro- and anti-inflammatory cytokines is associated with sterilization. PLoS Pathog. *11*, e1004603.

Gosselin, A., Monteiro, P., Chomont, N., Diaz-Griffero, F., Said, E.A., Fonseca, S., Wacleche, V., El-Far, M., Boulassel, M.R., Routy, J.P., et al. (2010). Peripheral Blood CCR4+CCR6+and CXCR3+CCR6+ CD4+ T Cells Are Highly Permissive to HIV-1 Infection. J. Immunol. *184*, 1604–1616.

Green, G.H., and Diggle, P.J. (2007). On the operational characteristics of the Benjamini and Hochberg False Discovery Rate procedure. Stat. Appl. Genet. Mol. Biol. *6*, e27.

Kagina, B.M., Mansoor, N., Kpamegan, E.P., Penn-Nicholson, A., Nemes, E., Smit, E., Gelderbloem, S., Soares, A.P., Abel, B., Keyser, A., et al. (2015). Qualification of a whole blood intracellular cytokine staining assay to measure mycobacteria-specific CD4 and CD8 T cell immunity by flow cytometry. J. Immunol. Methods *417*, 22–33.

Kalokhe, A.S., Adekambi, T., Ibegbu, C.C., Ray, S.M., Day, C.L., and Rengarajan, J. (2015). Impaired degranulation and proliferative capacity of Mycobacterium tuberculosis-specific CD8+ T cells in HIV-infected individuals with latent tuberculosis. J. Infect. Dis. *211*, 635–640.

Kulkarni, A., Kurle, S., Shete, A., Ghate, M., Godbole, S., Madhavi, V., Kent, S.J., Paranjape, R., and Thakar, M. (2017). Indian Long-term Non-Progressors Show Broad ADCC Responses with Preferential Recognition of V3 Region of Envelope and a Region from Tat Protein. Front. Immunol. *8*, 5.

Kuroda, M.J., Sugimoto, C., Cai, Y., Merino, K.M., Mehra, S., Araínga, M., Roy, C.J., Midkiff, C.C., Alvarez, X., Didier, E.S., and Kaushal, D. (2018). High Turnover of Tissue Macrophages Contributes to Tuberculosis Reactivation in Simian Immunodeficiency Virus-Infected Rhesus Macaques. J. Infect. Dis. *217*, 1865–1874.

Lawn, S.D., and Wilkinson, R.J. (2015). ART and prevention of HIV-associated tuberculosis. Lancet HIV *2*, e221–e222.

Lin, P.L., and Flynn, J.L. (2018). The End of the Binary Era: Revisiting the Spectrum of Tuberculosis. J. Immunol. *201*, 2541–2548.

Lin, L., Finak, G., Ushey, K., Seshadri, C., Hawn, T.R., Frahm, N., Scriba, T.J., Mahomed, H., Hanekom, W., Bart, P.A., et al. (2015). COMPASS identifies T-cell subsets correlated with clinical outcomes. Nat. Biotechnol. *33*, 610–616.

Mercer, F., Khaitan, A., Kozhaya, L., Aberg, J.A., and Unutmaz, D. (2014). Differentiation of IL-17-producing effector and regulatory human T cells from lineage-committed naive precursors. J. Immunol. *193*, 1047–1054.

Murray, L.W., Satti, I., Meyerowitz, J., Jones, M., Willberg, C.B., Ussher, J.E., Goedhals, D., Hurst, J., Phillips, R.E., McShane, H., et al. (2018). Human Immunodeficiency Virus Infection Impairs Th1 and Th17 Mycobacterium tuberculosis-Specific T-Cell Responses. J. Infect. Dis. *217*, 1782–1792.

Okoye, A.A., and Picker, L.J. (2013). CD4(+) T-cell depletion in HIV infection: mechanisms of immunological failure. Immunol. Rev. *254*, 54–64.

Pawlowski, A., Jansson, M., Sköld, M., Rottenberg, M.E., and Källenius, G. (2012). Tuberculosis and HIV co-infection. PLoS Pathog. *8*, e1002464.

Rakshit, S., Adiga, V., Nayak, S., Sahoo, P.N., Sharma, P.K., van Meijgaarden, K.E., Uk J, A.J., Dhar, C., Souza, G.D., Finak, G., et al. (2017). Circulating Mycobacterium tuberculosis DosR latency antigen-specific, polyfunctional, regulatory IL10^{+} Th17 CD4 T-cells differentiate latent from active tuberculosis. Sci. Rep. *7*, 11948.

Rakshit, S., Ahmed, A., Adiga, V., Sundararaj, B.K., Sahoo, P.N., Kenneth, J., D'Souza, G., Bonam, W., Johnson, C., Franken, K.L., et al. (2019). BCG revaccination boosts adaptive polyfunctional Th1/Th17 and innate effectors in IGRA+ and IGRA- Indian adults. JCI Insight *4*, e130540.

Riou, C., Bunjun, R., Müller, T.L., Kiravu, A., Ginbot, Z., Oni, T., Goliath, R., Wilkinson, R.J., and Burgers, W.A. (2016). Selective reduction of IFN-γ single positive mycobacteria-specific CD4+ T cells in HIV-1 infected individuals with latent tuberculosis infection. Tuberculosis (Edinb.) *101*, 25–30.

Roederer, M., Nozzi, J.L., and Nason, M.C. (2011). SPICE: exploration and analysis of post-cytometric complex multivariate datasets. Cytometry A *79*, 167–174.

Seki, R., and Nishizawa, K. (2016). Factors regulating Th17 cells: a review. Biomed. Res. Clin. Pract. *1*, 126–147.

Sreenath, K., Pavithra, L., Singh, S., Sinha, S., Dash, P.K., Siddappa, N.B., Ranga, U., Mitra, D., and Chattopadhyay, S. (2010). Nuclear matrix protein SMAR1 represses HIV-1 LTR mediated transcription through chromatin remodeling. Virology *400*, 76–85.

Thakar, M.R., Abraham, P.R., Arora, S., Balakrishnan, P., Bandyopadhyay, B., Joshi, A.A., Devi, K.R., Vasanthapuram, R., Vajpayee, M., Desai, A., et al. (2011). Establishment of reference CD4+ T cell values for adult Indian population. AIDS Res. Ther. *8*, 35.

Trinchieri, G. (2001). Regulatory role of T cells producing both interferon gamma and interleukin 10 in persistent infection. J. Exp. Med. *194*, F53–F57.

Vandergeeten, C., Fromentin, R., Merlini, E., Lawani, M.B., DaFonseca, S., Bakeman, W., McNulty, A., Ramgopal, M., Michael, N., Kim, J.H., et al. (2014). Cross-clade ultrasensitive PCR-based assays to measure HIV persistence in large-cohort studies. J. Virol. *88*, 12385–12396.

Volchenkov, R., Nygaard, V., Sener, Z., and Skålhegg, B.S. (2017). Th17 Polarization under Hypoxia Results in Increased IL-10 Production in a Pathogen-Independent Manner. Front. Immunol. *8*, 698.

WHO (2019a). Global Tuberculosis Report. https://www.who.int/tb/publications/global_report/en/.

WHO (2019b). HIV factsheets 2019. http://www.who.int/news-room/fact-sheets/detail/hiv-aids.

Yang, X., Jiao, Y.M., Wang, R., Ji, Y.X., Zhang, H.W., Zhang, Y.H., Chen, D.X., Zhang, T., and Wu, H. (2012). High CCR5 density on central memory CD4+ T cells in acute HIV-1 infection is mostly associated with rapid disease progression. PLoS ONE *7*, e49526.

Yang, B.H., Hagemann, S., Mamareli, P., Lauer, U., Hoffmann, U., Beckstette, M., Föhse, L., Prinz, I., Pezoldt, J., Suerbaum, S., et al. (2016). Foxp3(+) T cells expressing RORγt represent a stable regulatory T-cell effector lineage with enhanced suppressive capacity during intestinal inflammation. Mucosal Immunol. *9*, 444–457.

STAR★METHODS

KEY RESOURCES TABLE

REAGENT or RESOURCE	SOURCE	IDENTIFIER
Antibodies		
V450 Mouse Anti-Human IFN-γ	BD Biosciences	Cat# 560371 Clone: B27; RRID:AB_1645594
FITC Mouse Anti-Human TNF	BD Biosciences	Cat# 552889 Clone: MAb11; RRID:AB_394518
Alexa Fluor 700 anti-human IL-2	BioLegend	Cat# 500320 Clone: MQ1-17H12; RRID:AB_528929
Brilliant Violet 605 anti-human IL-17A	BioLegend	Cat# 512326 Clone: BL168; RRID:AB_2563887
Brilliant Violet 650 Mouse Anti-Human IL-17F	BD Biosciences	Cat# 564264 Clone: O33-782; RRID:AB_2869555
PE-Cy7 Mouse Anti-human IL-22	eBioscience	Cat# 25-7229-42 Clone: 22URTI; RRID:AB_10853346
Brilliant Violet 786 Rat Anti-Human and Viral IL-10	BD Biosciences	Cat# 564049 Clone: JES3-9D7; RRID:AB_2738563
PE Mouse Anti-Human MIP-1β	BD Biosciences	Cat# 550078 Clone: D21-1351; RRID:AB_393549
APC-H7 Mouse Anti-Human CD45RA	BD Biosciences	Cat# 560674 Clone: HI100; RRID:AB_1727497
Alexa Fluor 647 anti-human CCR7	BioLegend	Cat# 353218 Clone: G043H7; RRID:AB_10917385
Brilliant Violet 570 anti-human CD3	BioLegend	Cat# 300436 Clone: UCHT1; RRID:AB_2562124
BUV395 Mouse Anti-Human CD4	BD Biosciences	Cat# 563550 Clone: SK3;RRID:AB_2738273
Brilliant Violet 711 Mouse Anti-Human CD8	BD Biosciences	Cat# 563677 Clone: RPA-T8; RRID:AB_2744463
Alexa Fluor 488 anti-human CD45RA	BioLegend	Cat# 304114 Clone: HI100; RRID:AB_528816
PE-Cy7 anti-human CCR7	BioLegend	Cat# 353226 Clone: G043H7; RRID:AB_11126145
Brilliant Violet 510 anti-human CD14	BioLegend	Cat# 301842 Clone: M5E2; RRID:AB_2561946
Brilliant Violet 510 anti-human CD19	BioLegend	Cat# 302242 Clone: HIB19; RRID:AB_2561668
PE Mouse Anti-Human CD154	BD Biosciences	Cat# 555700 Clone: TRAP1; RRID:AB_396050
APC Mouse Anti-Human CD69	BD Biosciences	Cat# 340560 Clone: L78; RRID:AB_400523
CD40 antibody, Mouse Anti-human	Miltenyi Biotec	Cat# 130-094-133 Clone: HB14; RRID:AB_10839704
Biological Samples		
PBMC samples from HIV-IGRA-, HIV-IGRA+, HIV+IGRA-, HIV+IGRA+ subjects, Pulmonary and extrapulmonary TB before and after ATT	St. John's Medical College Hospital, Bangalore, India	N/A
PBMC samples from HIV+IGRA+, HIV+IGRA+LTNP individuals	National AIDS Research Institute, Pune, India	N/A

(*Continued on next page*)

Continued

REAGENT or RESOURCE	SOURCE	IDENTIFIER
Chemicals, Peptides, and Recombinant Proteins		
Histopaque 1077	Sigma Aldrich	Cat# 10771
Live/Dead Fixable Aqua Dead Cell Stain Kit	Invitrogen	Cat# L34966
ULtraComp eBeads	Invitrogen	Cat# 01-2222-42
Remel Phytohemagglutinin Purified	ThermoFisher Scientific	Cat# R30852801
SuperScript III Reverse Transcriptase	ThermoFisher Scientific	Cat# 18080093
ESAT6/CFP10 fusion protein	Department of Infectious Diseases, Leiden University Medical Center	N/A
Latency antigens (Rv1733c, RV1737c, Rv2029, RV2628)	Department of Infectious Diseases, Leiden University Medical Center	N/A
BD FastImmune CD28/CD49d Purified	BD Biosciences	Cat# 347690, Clone: L293/L25
Brefeldin A Solution (1,000X)	BioLegend	Cat# 420601
Monensin Solution (1,000X)	BioLegend	Cat# 420701
BD FACS Lysing Solution 10X Concentrate	BD Biosciences	Cat# 349202
BD Phosflow Perm/Wash Buffer I	BD Biosciences	Cat# 557885
Paraformaldehyde	Electron Microscopy Sciences	Cat# 15712-S
PepMix HCMVA (pp65)	JPT Peptide Technologies	Cat# PM-PP65-2
HIV-1 PTE Gag Peptide Pool 1	NIH AIDS Reagent Program	Cat# 12437
HIV-1 PTE-G Env Peptide Pool 1	NIH AIDS Reagent Program	Cat# 12698
Critical Commercial Assays		
TruCOUNT kit	BD Biosciences	Cat# 662415
Abbott RealTime HIV-1 Viral Load Assay	Abbott Molecular Inc.	Cat# 06L18-070
GAPDH Taq Man Gene Expression Assay (Hs99999905_m1)	ThermoFisher Scientific	Cat# 4351370
Taqman gene expression assay IFN-γ (Hs00989291_m1)	ThermoFisher Scientific	Cat# 4331182
Taqman gene expression assay IL-2 (Hs00174114_m1)	ThermoFisher Scientific	Cat# 4331182
Taqman gene expression assay MIP-1β (Hs99999148_m1)	ThermoFisher Scientific	Cat# 4331182
HIV GAG Custom TaqMan Probe Assay ID: AIHSQJI	ThermoFisher Scientific	Cat# 4331348
HIV-1 LTR Vanderg Custom TaqMan® Gene Expression Assay ID: APRWEWY	ThermoFisher Scientific	Cat# 4332078
HUM-CD3-Vanderg Custom TaqMan® Gene Expression Assay ID: APDJXRR	ThermoFisher Scientific	Cat# 4332078
Single Cell-to-CT qRT-PCR Kit	ThermoFisher Scientific	Cat# 4458236 & 4458237
Arcturus® PicoPure® DNA Extraction Kit	ThermoFisher Scientific	Cat# KIT0103
TaqMan Gene expression Master Mix	Applied Biosystems	Cat# 4369016
Amplitaq Gold 360 DNA Polymerase	Applied Biosystems	Cat# 4398823
Experimental Models: Cell Lines		
ACH-2 cells	Gift from Dr. Udaykumar Ranga, JNCASR, Bangalore.	Sreenath et al., 2010
HIV (pNL4-3 virus) infected Jurkat T cells	Gift from Dr. Udaykumar Ranga, JNCASR, Bangalore.	Sreenath et al., 2010
Software and Algorithms		
GraphPad Prism 8.0.2	GraphPad Software	https://www.graphpad.com/
FlowJo version 9.9.6	Becton, Dickinson & Company	https://www.flowjo.com/
FACS DIVA	BD Biosciences	http://www.bdbiosciences.com/en-us

(*Continued on next page*)

Continued

REAGENT or RESOURCE	SOURCE	IDENTIFIER
COMPASS	Lin et al., 2015	https://bioconductor.org/packages/COMPASS/
Pestle v1.8	Roederer et al., 2011	https://niaid.github.io/spice/
SPICE v5.1	Roederer et al., 2011	https://niaid.github.io/spice/
7000 System SDS Software v1.2.3	Applied Biosystems	http://tools.thermofisher.com/content/sfs/manuals/cms_039287.pdf

RESOURCE AVAILABILITY

Lead Contact

Further information and requests for resources and reagents should be directed to and will be fulfilled by the Lead Contact, Annapurna Vyakarnam (anna.vyakarnam@kcl.ac.uk).

Materials Availability

This study did not generate new unique reagents.

Data and Code Availability

This study did not generate any unique datasets or code.

EXPERIMENTAL MODEL AND SUBJECT DETAILS

Study population

This study was performed in accordance with the relevant guidelines and regulations stated in the 'Declaration of Helsinki' and approved by the ethical review Committee of St. John's Medical College Hospital, Bangalore, India (Ref no: 55/2015) and the institutional ethics review board of National AIDS Research Institute (NARI/EC Protocol No.: 2012–06). A total of 205 individuals were recruited at St. John's Medical College Hospital, Bangalore, India and 78 at National AIDS Research Institute, Bhosari, Pune, Maharashtra, India between April 2015 and June 2017. After proper counselling, all participants provided written informed consent before enrolment. Relevant clinical information was documented in a proforma and 40 ml blood was drawn from each enrolled individual by venepuncture in ACD, EDTA or heparin tubes depending on the immune assays. The demographic, immunological, and virological characteristics of the eight clinical groups are listed in Table 1. Detailed information of each participant has been included in Table S1.

HIV uninfected healthy IGRA$^+$ and IGRA$^-$ subjects

Healthcare workers of St. John's National Academy of Health Sciences were recruited through internal calls highlighting the nature and importance of the study. A commonly used interferon γ (IFN-γ) release assay (IGRA) for detecting *Mycobacterium tuberculosis* (Mtb) infection is the QuantiFERON-TB Gold In-tube test (QFT, QIAGEN, Germany) (Auguste et al., 2017). It involves culturing blood cells with Mtb-specific antigens ESAT6, CFP10 and TB7.7 that do not cross react with antigens present in BCG vaccine or other non-tuberculous mycobacteria. A positive result is considered predictive of infection with Mtb. The kit also includes a positive control for T cell activation and IFN-γ release (PHA) and a negative control (no antigen control) to adjust for spontaneous IFN-γ release. Study participants were screened based on this IGRA test and were stratified as IGRA$^+$ if their IFN-γ levels were greater than 0.35 IU/ml and IGRA$^-$ if the levels were below this cut-off. The detailed IGRA results have been summarized in the Supplemental Clinical File. All IGRA$^+$ subjects were asymptomatic for TB and had not received preventive/curative therapy for TB in the past. A total of 88 subjects were recruited and screened by the IGRA test, of which 26 were IGRA$^+$. Out of 26, 10 IGRA$^+$ subjects were included for the study; of which 80% were males with a median age of 30 years (25-38). Of the remaining 66, 10 IGRA$^-$ subjects served as uninfected healthy controls, of which 40% were males with a median age of 28 years (20-39). Healthcare workers in India do not undergo routine IGRA screening at the time of employment. Hence, ascertaining the duration for which our study subjects were IGRA$^+$ was not possible.

Pulmonary and Extrapulmonary TB

Subjects for this prospective study were enrolled at the Revised National Tuberculosis Program (RNTCP) clinic of St. John's Medical College and Hospital. According to the RNTCP guidelines, smear positivity is considered to be sufficient for diagnosis of pulmonary TB, chest radiograph and sputum culture is not necessary for TB diagnosis in India. Hence, diagnosis of pulmonary TB was ascertained by sputum smear microscopy and culture. Standard smear grading of 1^+, 2^+ and 3^+ was used to ascertain the bacterial burden. Smear negative cases of pulmonary TB cases were diagnosed and classified by the treating clinician from plain chest radiographs as per the RNTCP standards. GeneXpert MTB/RIF assay (Cephid, USA), a nucleic-acid amplification (NAA) test of tissue sample

approved by RNTCP, was used for confirmation of diagnosis. All patients included in the study were smear positive and positive for TB by GeneXpert. Rifampicin resistance by GeneXpert was an exclusion criterion. Sputum samples were collected for reconfirmation of TB diagnosis by GeneXpert MTB/RIF assay. Consenting adult patients meeting the above inclusion and exclusion criteria were included. A total of 5 cases of pulmonary TB were included in the study of which 80% were males with a median age of 34 years (30-66). A diagnosis of extrapulmonary TB was established from tissue specimens by Ziehl-Neelsen (ZN) staining for detection of AFB in tissue samples (obtained as surgical specimens/biopsies/FNACs). The site of extrapulmonary TB varied: 13 cases had cervical lymphadenitis and 2 had tubercular pleural effusions while the remaining four cases included one each of peritoneal TB, endometrial TB, intestinal TB and cold abscess. A total of 3 cases of extrapulmonary TB were included in the study of which 66.7% were males with a median age of 25 years (17-45). Study subjects were treatment naive at the time of enrolment and were counselled and initiated on standard anti-TB treatment (ATT) based on the directly observed treatment, short course (DOTS) regimen. Samples from 8 longitudinal donors (PTB, N = 5 and EPTB, N = 3) having undergone ATT for a period of 6 to 9 months were used in the study (Table 1). At a follow up visit 6-9 months from the start of ATT, blood was collected in EDTA or ACD tubes for isolation of PBMC.

HIV$^+$progressors, LTNP and HIV-TB coinfected patients

Subjects for this prospective study were enrolled at the ICMR-National AIDS Research Institute, Pune. HIV sero-positivity was confirmed by the standard HIV I and II ELISA test and western blot. CD4$^+$ T cell counts were estimated by flow cytometry (FACSCalibur, Becton Dickinson, USA) as a part of routine investigations using TruCOUNT kit (Becton Dickinson, USA) at baseline and following therapy. HIV-1 RNA viral loads (copy number/ml) were evaluated in the stored plasma samples using the Abbott Real Time HIV-1 viral load assay (Abbott Molecular Inc., Des Plaines, IL, USA) on the m2000 System (Roche diagnostics, Germany) at all study visits according to the manufacturer's instructions. HIV positive subjects attending the antiretroviral clinic, voluntary counseling and testing center of St John's Hospital and Medical College, Bangalore and National AIDS Research Institute, Pune were recruited prospectively into this study. Only subjects with no prior history of treatment on anti-retroviral drugs (ART naive) or post exposure prophylaxis were included. Patients having a CD4 count below 350 cells/mm^3 were initiated on anti-retroviral treatment. A thorough physical examination was carried out to rule out opportunistic infections and concomitant tuberculosis. Whole blood was collected in EDTA vacutainer tubes from each patient before ART administration for measuring HIV-1 viral load and drug resistance genotyping. Patients were followed up every 6 months with repeat blood draws for samples from treatment naive, confirmed HIV$^+$ subjects, negative for opportunistic infection and TB have been archived for this study with varying CD4 counts and virus loads. Progressors were defined as antiretroviral treatment (ART)-naive HIV-infected patients with a CD4 count below 400 cells/mm^3 and were also simultaneously tested for TB specific secretary IFN-γ release by IGRA (Interferon Gamma Release Assay). A total of 10 HIV$^+$IGRA$^+$ subjects were enrolled in the study of which 50% were males with a median age of 37.5 years (27-56). A total of 10 HIV$^+$IGRA$^-$ subjects were enrolled in the study of which 70% were males with a median age of 31 years (24-47). Long term non progressors (LTNP) were defined as individuals with asymptomatic HIV infection for 7 or more years who stably maintained their CD4 count above 500 cells/mm^3 in absence of ART (Kulkarni et al., 2017). The mean seropositivity in LTNP cohort was 10.8 years with a range from 7 to 19 years. The CD4 counts of LTNPs at the study visit (median 823 cells/μl [IQR 679–1259]) were significantly higher than HIV+ progressors (median 352 cells/μl [IQR 289–540]). As expected, the plasma viral load values at the study visits were significantly lower in LTNPs (median 9943 HIV RNA copies/ml [IQR 0–19897]) when compared to the values from progressors (median 27926 [IQR 3510–516564]) (Table 1). LTNP subjects selected were also confirmed to be IGRA$^+$. A total of 7 LTNP subjects were enrolled in the study of which 42.8% were males with a median age of 36.5 years (33-48). The above cohorts were maintained at National AIDS Research Institute. HIV-TB coinfected patients were recruited at the RNTCP clinic of St. John's Medical College and Hospital, of which 8 were used for the study and 87.5% were males with a median age of 37 years (23-67).

Sample collection and processing

Peripheral blood mononuclear cells (PBMC) isolated from blood samples within 3 hr of blood draw by Histopaque (Sigma) density gradient centrifugation were cryopreserved in freezing medium containing 90% fetal calf serum (FCS) and 10% dimethyl sulfoxide (DMSO) and stored in liquid nitrogen until further usage.

METHOD DETAILS

Intracellular cytokine staining (ICS) assay and multiparameter flow cytometry

ICS assay with antigen-stimulated PBMCs was performed as previously described (Rakshit et al., 2017). Briefly, cryopreserved PBMCs were thawed and seeded in 96-well round-bottom plates (Costar) at a concentration of 1 × 10^6 cells/well after 2hr of rest. Next, 1 μg/ml FastImmune CD28/CD49d (BD Biosciences) was added that enhances the cytokine production in CD4$^+$ T cells in response to protein antigens and peptides by amplifying the signal for T cell recognition (Kagina et al., 2015). Cells were either left unstimulated or stimulated overnight with antigens; 10 μg/ml of a pool of 4 DosR regulon-encoded LT Ag (Rv1733c, Rv1737c, Rv2029 and Rv2628) or secretory Mtb antigen ESAT6/CFP10 (EC) produced by Kees LMC Franken as recombinant proteins at the Department of Infectious Diseases, Leiden University Medical Center (Franken et al., 2000), 1.7 μg/ml CMVpp65 peptide pool (JPT Peptide Technologies) and 1 μg/ml Phytohemagglutinin (PHA, Remel), followed by addition of brefeldin A and monensin (1X, BioLegend) for the last 16 hr. Next day, PBMCs were first stained with Live/Dead fixable Aqua dead

cell stain or AviD (Invitrogen) to exclude dead cells from analysis, for 10 min at room temperature (RT). Details for all specific and titrated fluorochrome conjugated monoclonal antibodies to cell surface and intracellular markers used in the intracellular cytokine staining (ICS) assay are listed in the resource table. For analysis of T cell responses, cells were stained with cell surface antibodies to CD45RA-APC-H7 (HI100) and CCR7-Alexa Fluor 647 (G043H7). Cells were then fixed with 1X FACS lysis buffer (BD Biosciences) for 10 min and permeabilized with 1X BD Perm/Wash buffer (BD Biosciences) for 20 min. For staining of intracellular cytokines, cells were incubated with a cocktail containing antibodies to CD3-BV570 (UCHT1), CD4-BUV395 (SK3), CD8-BV711 (RPA-T8), IFN-γ-V450 (B27), TNF-α-FITC (MAb11), IL-2-Alexa Fluor 700 (MQ1-17H12), IL-17A-BV605 (BL168), IL-17F-BV650 (O33-782), IL-10-BV786 (JES3-9D7), IL-22-PE-Cy7 (22URTI) and MIP-1β-PE (D21-1351). Antibody incubations were all performed at RT for 30 min in the dark. Cells were washed, fixed in 1% paraformaldehyde and kept at 4°C until acquisition.

Flow cytometry and data analysis

Samples were analyzed by flow cytometry using on BD FACSAria™ Fusion flow cytometer (BD Biosciences, San Jose, CA) and the associated BD FACSDiva™ version 8.0.1 software Cytometer Setting and Tracking (CST) beads (BD Biosciences) were acquired before each experiment to ensure that cytometer parameters remained consistent across all experiments. Stained samples were acquired with a standard stopping gate set at 200,000 CD3 lymphocytes. Negative and single-stained compensation beads (eBioscience) were acquired for each experiment, before sample acquisition, and used to calculate the compensation matrix. Data were then analyzed using the FlowJo version 9.9.6 software (FlowJo), Pestle v1.8, SPICE v5.1 (Roederer et al., 2011) as described previously. Briefly, $CD4^+$ T cells expressing all possible combinations (256 subsets) of 8 effector cytokines were analyzed by Boolean gating in FlowJo. After careful analysis, the data were further analyzed by SPICE which identified 6 unique Th17 subsets that either expressed IFN-γ or IL-10 in combination with IL-17A/IL-17F/IL-22. These subsets were positive only for these cytokines and with no expression of other cytokines (IL-2, TNF-α and MIP-1β).

COMPASS analysis of flow cytometry data

Cell counts were analyzed using the COMPASS algorithm as described. Briefly, COMPASS is a statistical model developed for high-dimensional flow cytometry data analysis that can detect antigen-specific changes across all observable functional T cell subsets, without the need to limit the analysis to very specific subsets based on expected biological significance (Lin et al., 2015). In COMPASS, responses are quantified using posterior probabilities that summarize for each subject and subset the evidence that the corresponding response is Ag specific by comparing the proportion of cytokine-positive cells in the Ag sample to the corresponding proportion in the control sample. Polyfunctionality scores were calculated from posterior responses probabilities, summarizing a subject's entire T cell functionality profile into a single number. In this study, we have applied COMPASS to each of the antigens in $CD4^+$ T cell subsets leading to 20 analyses. Each one of the analyses was unbiased and considered all of the 256 possible cytokine functions (defined as Boolean combination). In order to evaluate differences in polyfunctionality between groups, a linear model estimating the group wise mean polyfunctionality scores was fit to each antigen and the difference between $IGRA^+$ and other groups was tested (Wald test, null:, two-sided test). Resulting p values were adjusted for multiple testing (across all 60 tests and models) to control the FDR (false discovery rate) using the method of Benjamini & Hochberg (Green and Diggle, 2007). Significant differences were called at the 5% FDR level. Magnitudes of T cell responses were calculated independent of COMPASS as the maximum of zero or the proportion of gated events in the stimulated condition minus the proportion of gated events in the unstimulated condition.

Capture of antigen-specific $CD4^+$ T cells

Cryopreserved PBMCs were thawed, rested for 2 hr and plated in U bottom 96 well plate at 1×10^6/ well., Cells were then blocked with 0.5 μg/ml CD40 (HB14) antibody for 15 min at 37°C. Blocking antibody to CD40 prevents CD154 downregulation and thereby facilitates capture of $CD154^+$ antigen specific $CD4^+$ T cells (Frentsch et al., 2005). Next, anti-CD28/CD49d costimulatory antibody and antigens (CMVpp65, EC, LT Ag and HIV-PTE (Env-1-3, and Gag 1-2) pools were added for 16 hr. Next day, PBMCs were stained with AviD the monoclonal antibodies to CD3-BV570 (UCHT1), CD4-BUV395 (SK3), CD8-BV711 (RPA-T8), CD45RA-Alexa Fluor 488 (HI100), CCR7-PE-Cy7 (G043H7), CD14-BV510 (M5E2), CD19-BV510 (HIB19), CD154-PE (TRAP1), CD69-APC (L78) listed in resource table and sorted on a BD FACSAria Fusion flow cytometer with a 100 μm nozzle, 15 psi, 100 rpm agitation at 4°C with a flow rate of 3000–6000 events/sec. Cells were sorted using FACS Diva software to isolate antigen-specific ($CD3^+CD4^+CD154^+CD69^+$) and resting ($CD3^+CD4^+CD154^-CD69^-$) $CD4^+$ T cells, referred to as $CD154^+CD69^+$ and $CD154^-CD69^-$ henceforth, for quantification of cell-associated HIV DNA and HIV RNA .

DNA isolation

DNA isolation was performed using Arcturus Pico Pure DNA kit (ThermoFisher Scientific) as per manufacturer's instructions. Isolated DNA was directly used in the pre-amplification PCR performed in the same tube for both HIV-1 LTR and human CD3 gene.

Real-Time Quantitative Reverse Transcription PCR PCR (qRT-PCR) for quantification of total cell-associated HIV DNA

Total cell associated HIV DNA was quantified by the method described previously (Vandergeeten et al., 2014) with some modifications. qRT-PCR was performed using custom synthesized HIV-1 LTR and human CD3 gene based TaqMan Gene expression assays and TaqMan Gene expression Master Mix (Applied Biosystems) on the StepOne Plus Real-Time PCR Detection System (Applied Biosystems) according to the manufacturer's recommendations. Before qRT-PCR, DNA prepared from sorted cells was subjected to pre-amplification PCR performed in single tube of 50 μL PCR reaction volume for both HIV-1 LTR and human CD3 gene using Amplitaq Gold 360 DNA Polymerase. The absolute quantity of cell associated HIV DNA was calculated based on standard curves of ACH-2 cells, which carry a single copy of the integrated HIV genome, which were used to generate standard curves for both HIV-1 LTR and human CD3 gene (Figure S7). Series of ten-fold dilutions of ACH-2 cells DNA corresponding to 3×10^5 to 3 HIV-1 DNA copies per reaction was included in each experiment in order to generate standard curves for both HIV-1 LTR as well as human CD3 gene. Individual standard curves from each experiment were used to determine the copy number of HIV-1 LTR and human CD3 gene respectively. All samples were analyzed in duplicate. The result of the cell associated HIV-1 DNA quantification was expressed as number of HIV DNA copies per million $CD4^+$ T cells. Two negative controls are typically included in each plate: DNase/RNase-free water, as a control for the PCR (no template control, NTC) and DNA extracted from the HIV uninfected Jurkat T cells. Additionally, DNA extracted from sorted $CD4^+$ T cells from PBMCs of HIV sero-negative healthy individuals were also included in few experiments to demonstrate the specificity of HIV-1 LTR qRT-PCR assay. DNA extracted from the HIV (pNL4-3 virus) infected Jurkat T cells was also included as positive control in each assay. Human CD3 gene was quantified in order to determine the input level of cellular DNA in the sample and was used as an endogenous reference to normalize variations due to differences in the cell count or DNA extraction. Total HIV DNA copies per million cells were determined by calculating the number of cells from the human CD3 gene copy number which is present as 2 copies of CD3 gene per cell.

Linearity, specificity and sensitivity of qRT-PCR assay to quantify cell-associated HIV DNA

The dynamic range of the assay for both HIV-1 LTR and Human CD3 gene encompassed at least 6 orders of magnitude, with a strong linear relationship ($r2 > 0.998$) between the Ct values and log10 input number of gene copies. HIV-1 LTR signal was never detected in any of the experiments in the negative control DNA (DNA of HIV negative Jurkat T cells and sorted CD4 T cells from PBMCs of HIV sero-negative healthy person) indicating the specificity of the qRT-PCR assay for HIV-1 LTR. For DNA from HIV negative Jurkat T cells the median CT value for human CD3 gene from 10 experiments was 22.36 (Range: 19.95 – 23.52) and no HIV-1 LTR signal was detected in any of the 10 experiments. When DNA of sorted CD4 T cells from PBMCs from HIV sero-negative healthy donor were tested in two experiments, the mean CT for human CD3 was 21.41 (SD 0.26) and no HIV-1 LTR signal was detected in both the experiments. Both human CD3 and HIV-1 LTR qRT-PCR assays were highly sensitive and could detect as low as single copy of the target gene in the 20 μL of template DNA used in the pre-amplification PCR reaction.

Relative quantification of cytokines and cell-associated HIV-1 RNA

Single Cell-to-CT kit was used to quantify cell-associated HIV-1 RNA. For each stimulation 100 to 250 cells ($CD154^+CD69^+$ or $CD154^-CD69^-$) were directly sorted into 10μl single cell lysis solution containing 1μl of single cell DNase I. Single Cell Stop solution (1μl) was added to stop the lysis reaction, followed by a 2min incubation at RT prior to freezing at −20°C. cDNA synthesis and pre-amplification were done according to manufacturer's instructions. TaqMan Probes used for pre-amplification (and later used for qRT-PCR) were: GAPDH (reference gene, Hs99999905_m1), GAG mRNA (in-house custom designed), IFN-γ (Hs00989291_m1), IL-2 (Hs00174114_m1) and MIP-1β (Hs99999148_m1). After pre-amplification, the samples were stored at −20°C. For gene expression analysis of the cDNA, a downscaled version of the qRT-PCR protocol supplied with the Single Cell-to-CT kit was used, with reactions performed in 10μl, comprising of 5μl 2X TaqMan Gene Expression Master Mix supplied with the kit, 5 times diluted cDNA sample, 0.5μl of 20X TaqMan probes and nuclease-free water. All qRT-PCR reactions were performed in a 96-well plate (Eppendorf), in duplicate and Cq values were averaged. Relative copy number (RCN_{gene}) was calculated against CT values of GAPDH mRNA levels in each sample (Equation 1). All the gene expressions (GAG, IFN-γ, IL-2 and MIP-1β are represented as Fold Change (FC_{gene}, Equation 2) by dividing RCN_{gene} by the median RCN of the same genes from unstimulated cells ($RCN_{med.unstimulated}$). Data are represented irrespective of the sorted $CD4^+$ cell type.

$$RCN_{gene} = power\left(2,^{-(\Delta CTgene - \Delta CTGAPDH)}\right) \quad (1)$$

$$FC_{gene} = RCN_{gene} / RCN_{med.unstimulated} \quad (2)$$

Clinical subjects with GAPDH CT in the range of 15 to 27 were considered. In order to confirm that the CT values for GAG-gene were indeed equivalent to actual gene expression and not any non-specific signal, control experiments were carried out using uninfected PBMCs and 250 cells were sorted for unstimulated and antigen-stimulated cells. qRT-PCR was carried out on these samples for the above mentioned TaqMan probes. The GAG gene RCN of uninfected PBMCs were considered to be non-specific binding (background noise) of TaqMan probe and clinical subjects with GAG gene CT to be greater than 32 were removed and GAG gene CT equivalent to undetermined were given a CT of 32 for further statistical analysis.

QUANTIFICATION AND STATISTICAL ANALYSIS

All antigen-stimulated wells were adjusted for non-specific responses by background subtraction (media alone). Statistical analyses were performed and graphs were created using GraphPad Prism software version 6.0.7 (GraphPad, La Jolla, CA). Paired longitudinal comparisons within the same group were done using the Wilcoxon matched-pairs signed rank test. Comparisons across two treatment groups were done using unpaired Mann–Whitney test. The p values were reported unadjusted, but were interpreted after adjustment using the Bonferroni correction for multiple comparisons. Statistical analyses across seven clinical groups was performed using a one-way ANOVA nonparametric Kruskal–Wallis test and corrected by Dunn's test for multiple comparisons.